CHEMISTRY

A EUROPEAN JOURNAL

Reprint

WILEY-VCH

EUChemSoc

CHEMISTRY
A EUROPEAN JOURNAL

GERMANY · NETHERLANDS · BELGIUM · ITALY · FRANCE · SPAIN · PORTUGAL · GREECE · CZECH REP. · POLAND

REPRINT

Ferrocene Peptides

L. Barišić, M. Čakić, K. A. Mahmoud, Y.-n. Liu, H.-B. Kraatz, H. Pritzkow, S. I. Kirin,* N. Metzler-Nolte,* V. Rapić** ..... 4965 – 4980

Helically Chiral Ferrocene Peptides Containing 1′-Aminoferrocene-1-Carboxylic Acid Subunits as Turn Inducers

2006 – 12/19

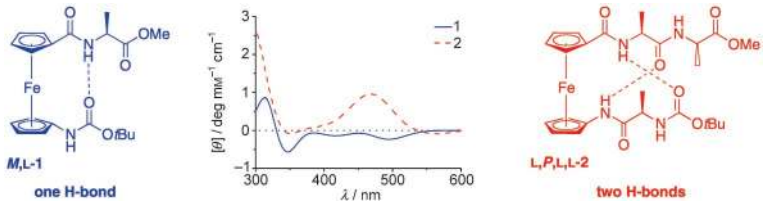

Turning point: Ferrocene amino acid (Fca) was incorporated into peptides with D- and L-alanine residues on the carboxy or amino group, or both. The helical chirality of ferrocene depends on the chirality of the amino acid at the N terminus of Fca (CD spectra, center). The degree of substitution of both Cp rings determines the H-bonding patterns. In dipeptides with one intramolecular H-bond (**1**), H-bonded and open forms are in equilibrium. Higher peptides, such as tetrapeptide **2**, form two intramolecular H-bonds stabilizing a single conformation.

SWEDEN · HUNGARY · AUSTRIA

WILEY-VCH

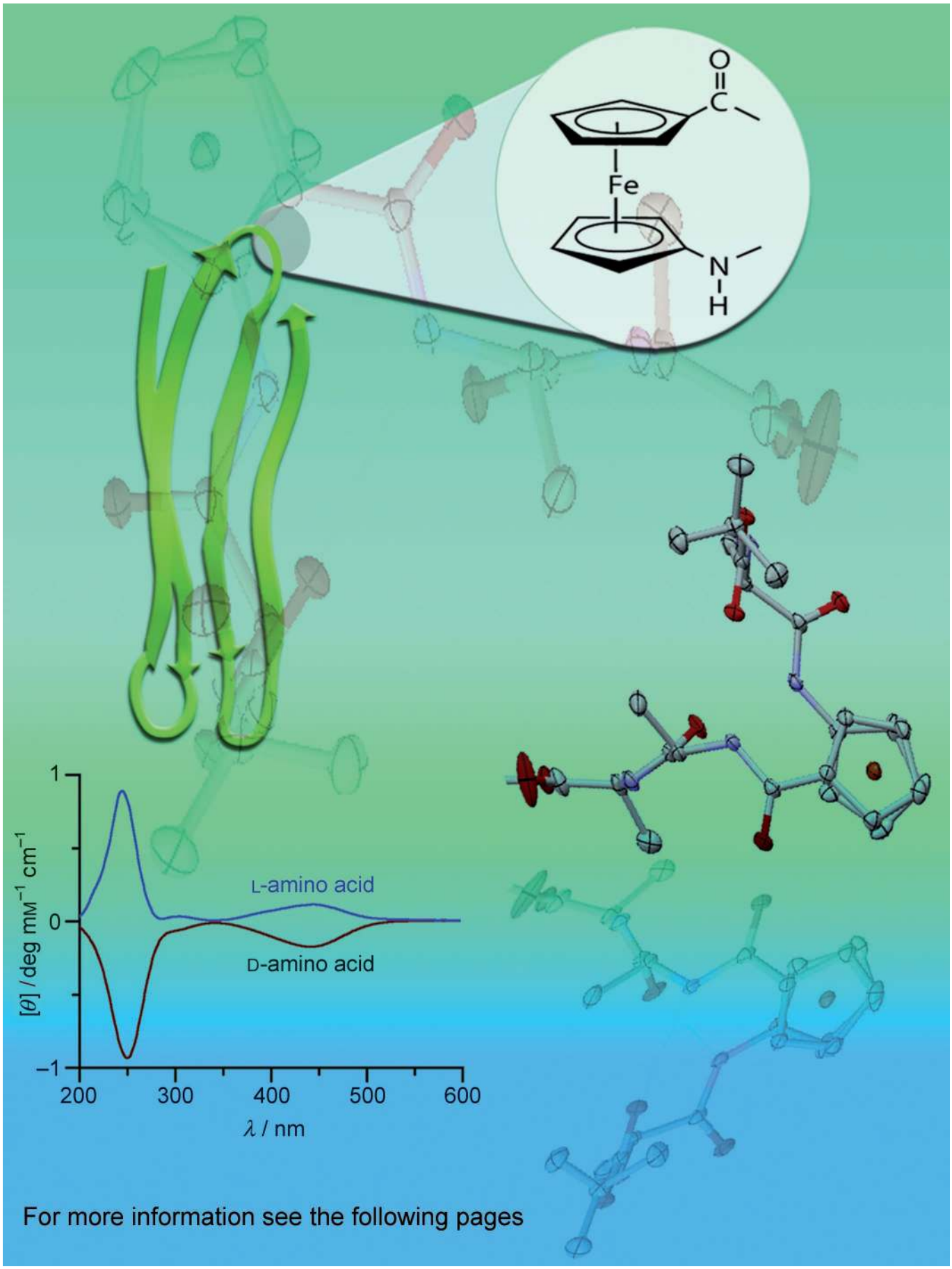

CHEMISTRY
A EUROPEAN JOURNAL

DOI: 10.1002/chem.200600156

Helically Chiral Ferrocene Peptides Containing 1′-Aminoferrocene-1-Carboxylic Acid Subunits as Turn Inducers

Lidija Barišić,[a] Mojca Čakić,[a] Khaled A. Mahmoud,[b] You-nian Liu,[b, f] Heinz-Bernhard Kraatz,*[b] Hans Pritzkow,[c] Srećko I. Kirin,*[d] Nils Metzler-Nolte,*[d, e] and Vladimir Rapić*[a]

Abstract: We present a detailed structural study of peptide derivatives of 1′-aminoferrocene-1-carboxylic acid (ferrocene amino acid, Fca), one of the simplest organometallic amino acids. Fca was incorporated into di- to pentapeptides with D- and L-alanine residues attached to either the carboxy or amino group, or to both. Crystallographic and spectroscopic studies (circular dicroism (CD), IR, and NMR) of about two dozen compounds were used to gain a detailed insight into their structures in the solid state as well as in solution. Four derivatives were characterized by single-crystal X-ray analysis, namely Boc-Fca-Ala-OMe (**16**), Boc-Fca-D-Ala-OMe (**17**), Boc-Fca-β-Ala-OMe (**18**), and Boc-Ala-Fca-Ala-Ala-OMe (**21**) (Boc = *tert*-butyloxycarbamyl). CD spectroscopy is an extremely useful tool to elucidate the helical chirality of the metallocene core. Unlike in all other known ferrocene peptides, the helical chirality of the ferrocene is governed solely by the chirality of the amino acid attached to the N terminus of Fca. Depending on the degree of substitution of both cyclopentadiene (Cp) rings, different hydrogen-bonding patterns are realized. ^{1}H NMR and IR spectroscopy, together with the results from X-ray crystallography, give detailed information regarding not only the hydrogen-bonding patterns of the compounds, but also the equilibria between different conformers in solution. Differences in chemical shifts of NH protons in dimethyl sulfoxide ([D$_6$]DMSO) and $CDCl_3$, that is, the variation ratio (vr), is used for the first time as a measure of the hydrogen-bonding strength of individual CO···HN bonds in ferrocenoyl peptides. In dipeptides with one intramolecular hydrogen bond between the pendant chains, for example, in dipeptide **16**, an equilibrium between hydrogen-bonded and open forms is observed, as testified by a vr value of around 0.5. Higher peptides, such as tetrapeptide **21**, are able to form two intramolecular hydrogen bonds stabilizing one single conformation in $CDCl_3$ solution (vr $\approx$0). Due to the low barrier of Cp-ring rotation, new and unnatural hydrogen-bonding patterns are emerging. The systematic work described herein lays a solid foundation for the rational design of metallocene peptides with unusual structures and properties.

Keywords: amino acids · bioorganometallic chemistry · ferrocene · hydrogen bonds · peptides

Introduction

The ability to control the secondary structure of peptides is one of the key requirements for the systematic design of functional peptide materials that can either be responsive to external stimuli or have properties[1] desirable for applications in bioelectronics or biophotonics. In addition, it in-

[a] Dr. L. Barišić, M. Čakić, Prof. Dr. V. Rapić
Faculty of Food Technology and Biotechnology
Pierottijeva 6, HR-10000 Zagreb (Croatia)
Fax: (+385) 1-4836-082
E-mail: vrapic@pbf.hr

[b] K. A. Mahmoud, Dr. Y.-n. Liu, Prof. Dr. H.-B. Kraatz
Department of Chemistry, University of Saskatchewan
110 Science Place, Saskatoon, Saskatchewan S7N 5C9 (Canada)
Fax: (+1) 306-966-4730
E-mail: kraatz@skyway.usask.ca

[c] Dr. H. Pritzkow
Anorganisch-Chemisches Institut der Universität Heidelberg
Im Neuenheimer Feld 270, 69120 Heidelberg (Germany)

[d] Dr. S. I. Kirin, Prof. Dr. N. Metzler-Nolte
Institut für Pharmazie und Molekulare Biotechnologie
Universität Heidelberg
Im Neuenheimer Feld 364, 69120 Heidelberg (Germany)
Fax: (+49) 6221-54-6441

[e] Prof. Dr. N. Metzler-Nolte
New address:
Lehrstuhl für Anorganische Chemie 1, Bioanorganische Chemie
Ruhr-Universität Bochum
Universitätsstrasse 150, 44801 Bochum (Germany)
Fax: (+49) 234-32-14378
E-mail: nils.metzler-nolte@rub.de

[f] Dr. Y.-n. Liu
On leave from:
College of Chemistry and Chemical Engineering
Central South University, Changsha, Hunan 410083 (China)

creases our understanding of naturally occurring proteins and enzymes.[2]

The use of molecular scaffolds is a common strategy to impart a specific secondary structure to a peptide backbone. For example, bipyridine–peptide conjugates adopt a β-sheet conformation upon the addition of Cu^{2+}, which coordinates to the bipy group and brings about significant structural changes that ultimately lead to the interstrand hydrogen-bonding and sheet formation. Other scaffolds hold great promise to induce specific turns, such as heterocyclic systems that impose rigidity to the peptide backbone. In this context, ferrocene derivatives are widely used as a redox-active scaffold.[3] The two cyclopentadiene (Cp) rings are separated by about 3.3 Å, which is ideal for interstrand hydrogen-bonding interactions, as was first proposed by Herrick and co-workers.[4] The particular choice of the ferrocene scaffold influences the ability to form hydrogen-bonded assemblies. For example, conjugates of ferrocenecarboxylic acid (FcCOOH) often give rise to one-dimensional hydrogen-bonded chains, whereas ferrocene-1,1′-dicarboxylic acid can give rise to a hydrogen-bonded β-sheet-like structure or even engage in chiral helical arrangements (Figure 1).[5–10]

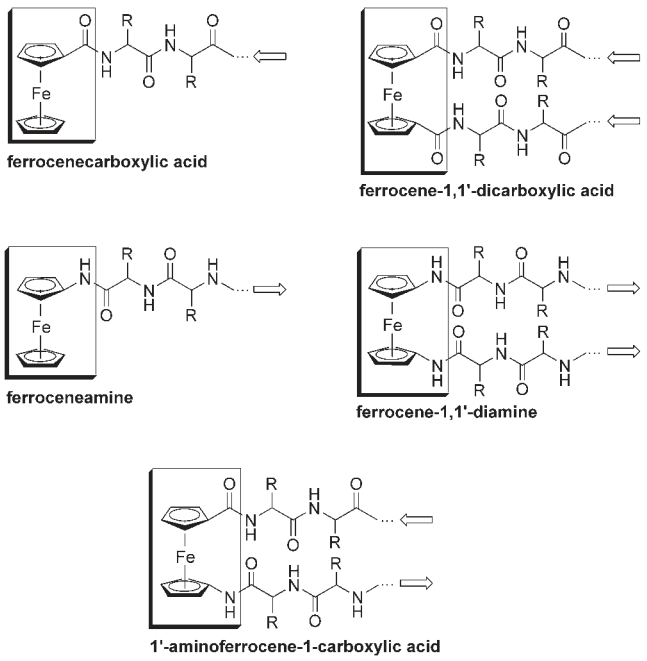

Figure 1. The ferrocene-derived peptide family. Arrows point from the C to the N termini of the peptides.

Recently, the use of more-rigid cystamine cyclopeptides based on ferrocene-1,1′-dicarboxylic acid and ferrocene-1,1′-diamine building blocks have allowed the isolation of systems able to engage in well-defined intermolecular hydrogen-bonding.[11] A derivative of ferrocene-1,1′-dicarboxylic acid was used as a transition-state analogue in an antibody-catalyzed Diels–Alder reaction.[12] The same group reported an early synthesis of 1′-aminoferrocene-1-carboxylic acid ("ferrocene amino acid"; Fca).[12a,13]

We reported recently on the efficient synthesis of Fca,[14a] which can be readily coupled to amino acids and peptides to give the corresponding Fca bioconjugates,[15] and induces the formation of a peptide turn. We have also reported on other Fca derivatives.[14b–d] We now expand our initial investigations and demonstrate the use of Fca to impose specific secondary-structural elements onto the peptide and present systematic spectroscopic (circular dicroism (CD), NMR, and IR) as well as crystallographic conformational analysis.

Results and Discussion

Synthesis: Syntheses of compounds **2**, **3**, **5**, and **7**–**10**, which serve as reference compounds in the following discussions, are depicted in Scheme 1. Activation of ferrocenecarboxylic acid **1** by 1-hydroxybenzotriazole (HOBt)/*N*-(3-dimethylaminopropyl)-*N*′-ethylcarbodiimide hydrochloride (EDC) in solution followed by coupling with CH_3NH_2 or H-Ala-OMe gave *N*-methylferrocenecarboxamide **2** and Fc-CO-Ala-OMe **3**, respectively. Ester **3** was hydrolyzed quantitatively into the free acid **4** according to the procedure published by Kraatz and co-workers,[8c] and was then coupled to H-Ala-OMe to give Fc-CO-Ala-Ala-OMe **5**.

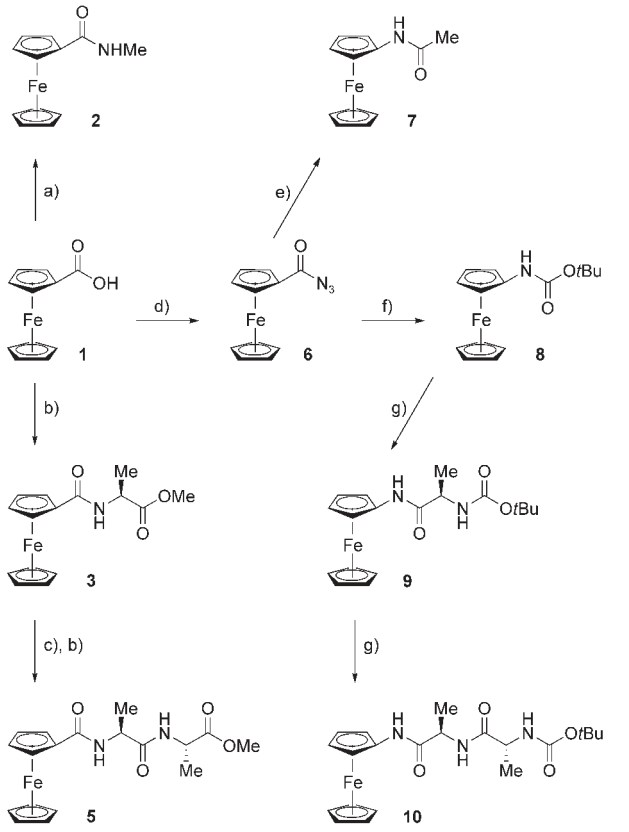

Scheme 1. Synthesis of the reference compounds. a) 1. EDC/HOBt, CH_2Cl_2, 2. CH_3NH_2·HCl/NEt_3, CH_2Cl_2; b) 1. EDC/HOBt, CH_2Cl_2, 2. H-Ala-OMe·HCl, CH_2Cl_2; c) NaOH, dioxane/H_2O; d) 1. ClCOOEt/NEt_3, acetone, 2. NaN_3, H_2O; e) Ac_2O; f) *t*BuOH; g) 1. HCl (gas)/EtOAc, 2. EDC/HOBt, CH_2Cl_2, 3. Boc-Ala-OH, CH_2Cl_2.

Alternatively, ferrocenecarboxylic acid **1** can be converted to the azide **6** in the presence of Et_3N, ClCOOEt, and NaN_3.[13] N-protected amides **7** (25%) and **8** (68%) were obtained by Curtius rearrangement of the azide **6** in Ac_2O or *t*BuOH solutions, respectively. Deprotection of Boc-NH-Fc **8** (Boc = *tert*-butyloxycarbamyl) was performed by the action of gaseous HCl in EtOAc. The resulting hydrochloride was treated with excess NEt_3 and coupled with Boc-Ala-OH to give 61% of Boc-Ala-NH-Fc **9**, which was treated analogously to compound **8** to obtain dipeptide Boc-Ala-Ala-NH-Fc **10** in quantitative yield.

The syntheses of the peptide analogues **12** and **15** are depicted in Scheme 2. The starting compounds **11** and **13** were

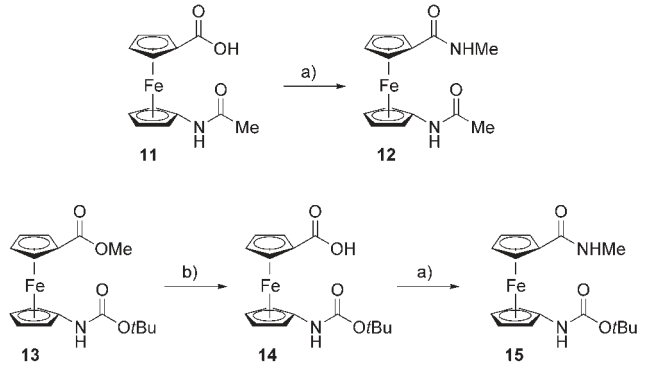

Scheme 2. Synthesis of the peptide analogues. a) 1. EDC/HOBt, CH_2Cl_2, 2. CH_3NH_2·HCl/NEt_3, CH_2Cl_2; b) NaOH, H_2O/MeOH.

prepared by the procedures described previously.[14a] Coupling of **11** with CH_3NH_2 by using the HOBt/EDC protocol results in formation of the diamide **12**. Hydrolysis of ester **13** gave 1′-(*tert*-butoxycarbonylamino)ferrocene-1-carboxylate (**14**, Boc-Fca-OH), which was transformed into the amide-carbamate **15** in a manner described for the preparation of compound **12**.

The preparation of the Fca-peptide conjugates **16**–**28** starting from Boc-Fca-OH **14** is summarized in Scheme 3. Firstly, the acid terminus of Fca was activated by HOBt and EDC and coupled with L-, D-, β-Ala, and H-Ala-Ala-OMe resulting in the formation of the C-terminal peptide conjugates **16** (74%), **17** (75%), **18** (79%), and **19** (76%), respectively.

Peptides **16** and **17** can be N-modified after Boc-deprotection of the organometallic core, followed by coupling with Boc-Ala-OH and Boc-D-Ala-OH to give the tripeptides **20** (72%) and **23** (72%), respectively. In a similar manner, dipeptide **17** was coupled with Boc-Ala-OH to yield tripeptide **24** (78%), and tripeptide **19** was coupled with Boc-$(Ala)_y$-OH, resulting in formation of the tetrapeptide **21** ($y = 1$) and the pentapeptide **22** ($y = 2$), respectively. The peptide can be elongated from the C- or the N-terminal side, followed by coupling with the desired amino-acid derivative. To demonstrate this approach, compound **25** was prepared from tripeptide **20**, and tetrapeptide **26** was prepared from **23**. N-Deprotection of compound **25**, followed by coupling with

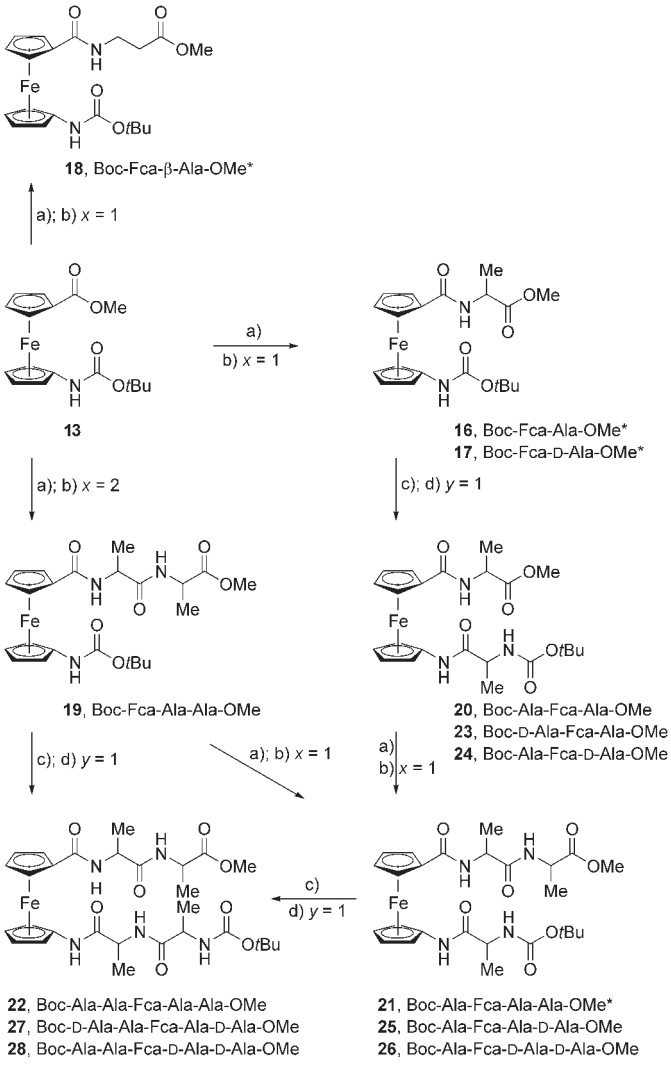

Scheme 3. Syntheses of Fca peptides. a) 1 M NaOH; b) 1. EDC/HOBt or HBTU/HOBt, CH_2Cl_2, 2. H-$(Aaa)_x$-OMe·HCl/NEt_3, CH_2Cl_2; c) HCl (gas)/EtOAc or TFA; d) 1. EDC/HOBt or HBTU/HOBt, CH_2Cl_2, 2. Boc-$(Aaa)_y$-OH/NEt_3, CH_2Cl_2. X-ray structures were obtained for compounds marked *.

Boc-D-Ala-OH by using O-(benzotriazole-1-yl)-*N*,*N*,*N*′,*N*′-tetramethyl-uronium hexafluorophosphate (HBTU)/HOBt results in formation of the pentapeptide **27**. Analogously, N-terminal-coupling of Boc-D-Ala-OH with compound **26** results in formation of the pentapeptide **28**.

Crystallographic analysis: Single crystals suitable for X-ray analysis were obtained for four compounds in this study. Peptides **16** and **21** were crystallized by slow diffusion of pentane into a solution of the compounds in chloroform ($\gamma = 10\ mg\,mL^{-1}$). Slow evaporation of an ether/heptane solvent mixture (3:1, $\gamma = 2\ mg\,mL^{-1}$) was successful for **17** and **18**. ORTEP diagrams of these compounds are shown in Figures 2–5. Although the intramolecular hydrogen-bonding patterns differ significantly (see below), the structures show a similar intermolecular hydrogen-bonding pattern. All four compounds crystallize in the $P2_12_12_1$ space group and build

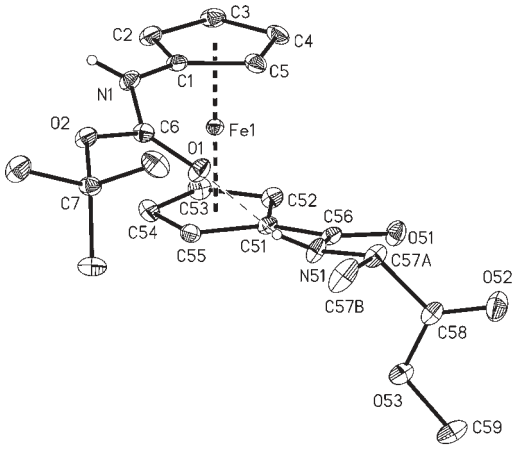

Figure 2. Crystal structure of dipeptide **16** showing L,*M* stereochemistry with one 8-membered hydrogen-bonded ring. (L: L-Ala, *M*: helical chirality of Fc core.)

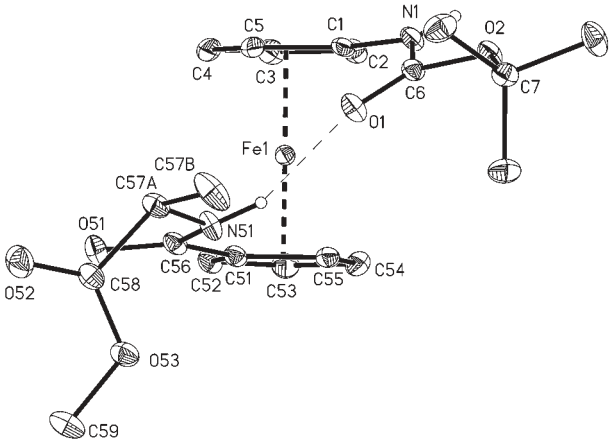

Figure 3. Crystal structure of dipeptide **17** showing D,*P* stereochemistry with one 8-membered hydrogen-bonded ring. (D: D-Ala, *P*: Fc helical chirality.)

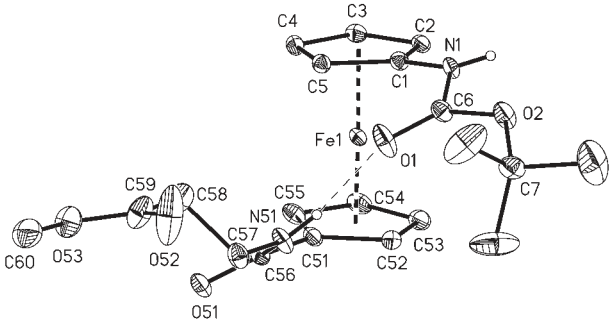

Figure 4. Crystal structure of dipeptide **18** showing *P* conformation with one hydrogen bond forming an 8-membered ring. Peptide **18** is a racemic (*M*/*P*) mixture, the *P* isomer was selected by chance.

chains along the crystallographic *c* (**16**, **17**, and **21**) or *b* axis (**18**), connected through one hydrogen bond, as exemplified for dipeptide **16** in Figure 6.

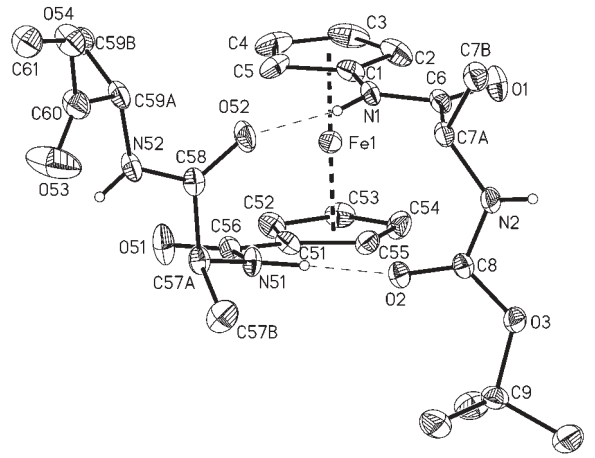

Figure 5. Crystal structure of tetrapeptide **21** showing L,*P*,L,L stereochemistry with 9- and 11-membered hydrogen-bonded rings (three L-Ala units forming a *P* helical conformer of Fc).

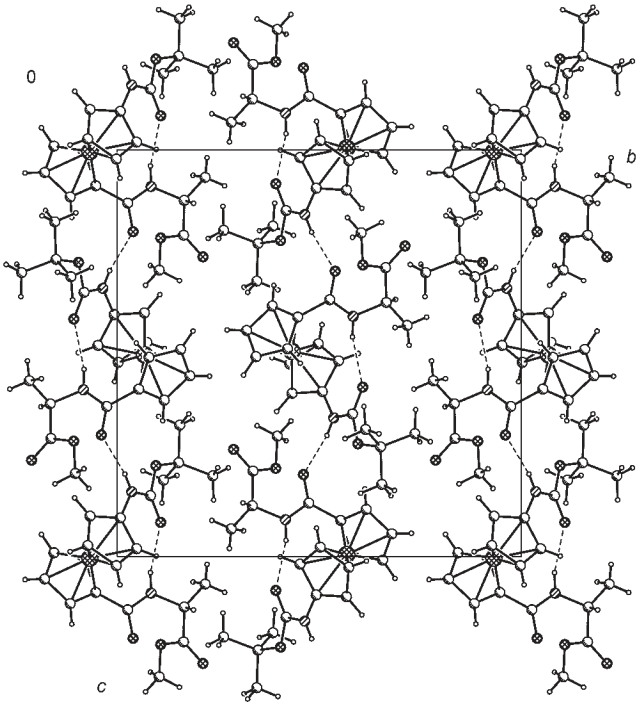

Figure 6. Crystal packing of dipeptide **16**, viewed down the crystallographic *a* axis.

The tetrapeptide **21** displays the peptide substituents in the 1 and 2′ positions and has two intramolecular interstrand hydrogen bonds (Figure 5).[15] Detailed conformational analysis revealed that the 1,2′-disubstituted ferrocene peptides can differ by the relative orientation of the NH and CO groups that are attached directly to the Cp rings: These groups can "point in" towards the cleft between the two substituents or "point out".[5b] Accordingly, different hydrogen bonds may form between the two peptide strands. This approach gives four possible conformers for a given 1,2′-di-

substituted ferrocene peptide, as shown for tetrapeptide **21** (Figure 7).

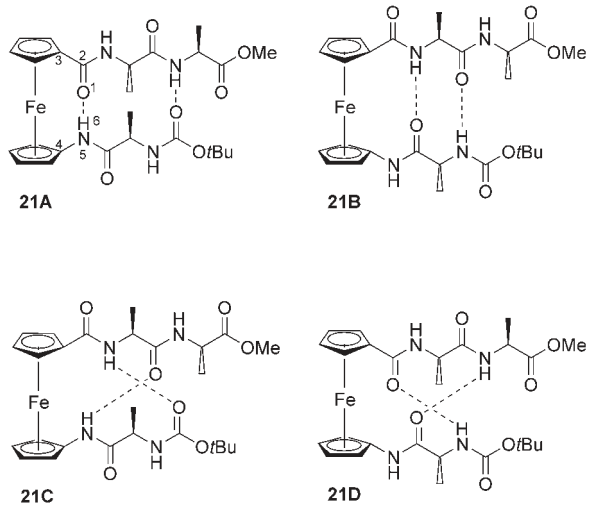

Figure 7. Possible intramolecular hydrogen-bonding pattern in tetrapeptide **21**. The numbering scheme for the specification of ring size in the hydrogen-bonded species is exemplified for conformer **A**.

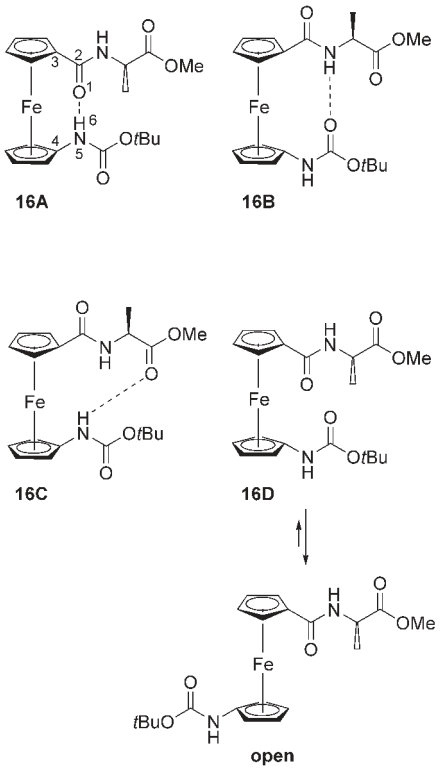

Figure 8. Possible hydrogen-bonding pattern in dipeptide **16**. The pattern **D** has no intramolecular hydrogen bonds and would exist as an "open isomer". The numbering scheme for the specification of ring size in the hydrogen-bonded species is exemplified for conformer **A**.

Table 1. Selected parameters in the crystal structures of **16**–**18** and **21**.

Parameter	**16**	**17**	**18**	**21**
N51–O1 [Å] [a]	2.90	2.90	2.81	–
N51–O2 [Å] [a]	–	–	–	2.91
N1–O52 [Å] [a]	–	–	–	2.81
N1–O51 [Å] [b]	2.86	2.86	2.91	–
N52–O1 [Å] [b]	–	–	–	2.96
θ [°]	2.0	1.9	3.8	3.0
β_{NH} [°]	29.6	29.7	23.5	6.3
β_{CO} [°]	9.3	9.3	33.9	5.4
ω [°]	85.1	85.0	77.9	60.7
angle sum around N1 [°]	359.7	359.8	357.9	359.2
angle sum around N2 [°]	–	–	–	359.9
angle sum around N51 [°]	352.1	353.9	358.5	359.4
angle sum around N52 [°]	–	–	–	359.9

[a] Intramolecular hydrogen bond. [b] Intermolecular hydrogen bond.

Initially, conformer **21B** was expected, with an 8-membered ring next to the ferrocene moiety. This conformer could be called "β-sheet-like", as it resembles a β-sheet with antiparallel strands and would facilitate the use of peptides derived from Fca as β-sheet models. However, surprisingly, conformer **21C** was found in the crystal of **21**, with two hydrogen bonds forming one 9-membered and one 11-membered ring (Figures 5 and 7). The stereochemistry of **21** is L,*P*,L,L, in which the three L describe the stereochemistry of the Ala residues and *P* describes the helical chirality of the ferrocene moiety.

Although the enantiomeric dipeptides **16** and **17** were crystallized from different solvents (see above), the same conformation was obtained. They represent the first examples in which the "β-sheet-like" conformer **B** was found in the solid state (Figures 2, 3, and 8). The stereochemistry is L,*M* for **16** and D,*P* for **17**, with one 8-membered intramolecular hydrogen bond. The similar *P* conformer was obtained for the β-alanine derivative **18** (Figure 4). Because **18** is achiral, a racemic mixture of *M* and *P* helical isomers was formed. Both isomers crystallized separately from this mixture and for the X-ray analysis a crystal of the *P* isomer was selected by chance.

Bond lengths and angles measured in the X-ray structures of **16**–**18** and **21** are within the expected range. A number of more significant structural parameters is collected in Table 1 and explained in Figure 9. In all four compounds, the two Cp rings are almost parallel to each other and consequently, the tilt angles are very small, $\theta < 4°$. The ω angles are close to the ideal value for a 1,2′-conformation ($360°/5 = 72°$) in all cases. A more interesting parameter is provided by the dihedral angle β and the pyramidalization of the amide nitrogen atoms. In tetrapeptide **21**, both amide groups are almost coplanar with the corresponding Cp rings ($\beta \sim 6°$) and the amide nitrogen atoms are not pyramidalized. This indicates the lack of steric strain of the ferrocene moiety, resulting in a favorable overlap between the π-systems of the amide and Cp groups. However, dipeptides **16**–**18** have some strain. At the -CO-NH-Cp side a clear indication is the large dihedral angle $\beta_{NH} > 20°$. At the Cp-CO-NH- side, β_{CO} is greater than 20° only in β-Ala compound **18**. In L-Ala conjugate **16** and D-Ala compound **17** the β_{CO} is about 10°, however, the sum of angles around the amide nitrogen atom

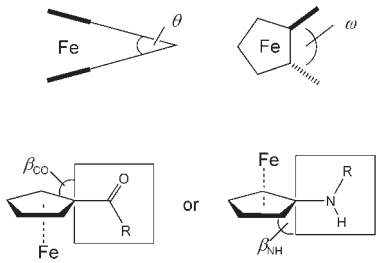

Figure 9. Tilt angle θ is the dihedral angle between the two Cp rings; ω is the dihedral angle between the two ring-bound substituents: C(*ipso*)-Cp-(centroid)-Cp(centroid)-C(*ipso*); β is the dihedral angle between the Cp ring and the -NHR (β_{NH}) or -COR′ (β_{CO}) substituent.

N51 is only about 353°. It can be concluded that the two hydrogen bonds in tetrapeptide **21** are easily formed and do not cause any sterical strain. On the contrary, dipeptides **16**–**18** have to accommodate some sterical hindrance to gain stabilization energy from the formation of one "β-sheet-like" hydrogen bond.

CD spectroscopy: As established from the crystallographic analyses of dipeptides **16**–**18** and tetrapeptide **21**, intramolecular hydrogen bonds are present in the solid state. This raises the question of whether the hydrogen-bonded structure persists in solution. CD spectroscopy was used for conformational analysis of the ferrocene peptides **16**–**28** in CH_3CN solution. CD signals between 300–600 nm are characteristic for metal-centered transitions. In particular, the band at 480 nm was described as a strong indication for a helically chiral ferrocene moiety.[5b] Molar ellipticities, $[\theta]$, were used to facilitate a comparison between different compounds.

The CD spectra of ferrocene dipeptides **16**–**18** and the tripeptide **19**, all substituted at the C terminus only, are displayed in Figure 10. As expected, the CD spectra of enantiomers **16** and **17** are a mirror image of each other. The L,*M*-derivative **16** displays a negative CD signal for the lowest-energy band at about 500 nm, whereas this signal is positive for D,*P*-**17**. Dipeptide **18**, containing the achiral β-alanine subunit, displays no CD signal in the ferrocene region because a racemic mixture of *M* and *P* conformers is present. Tripeptide **19**, with two L-Ala subunits on the C terminus of the Fca, shows a different pattern with significantly weaker CD signals than those of **16**.

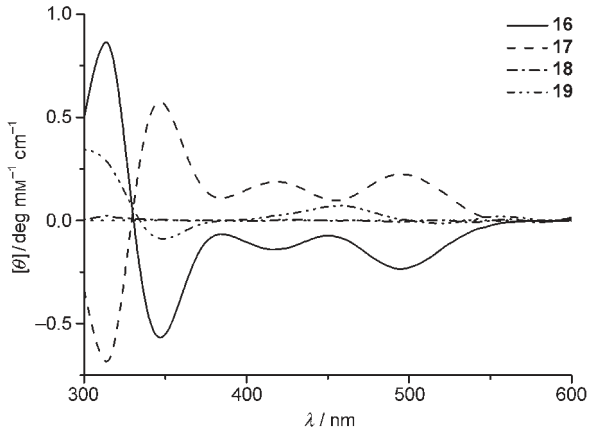

Figure 10. CD spectra (CH_3CN) of the dipeptides **16**–**18** and the tripeptide **19**.

The CD spectra of higher Fca peptides are shown in Figure 11 with the examples of compounds **20**, **23**, **24**, and **28**. All spectra of the ferrocene peptides **20**–**28** are qualitatively alike in the region above 400 nm with one signal centered at 480 nm, and differ significantly from the dipeptide **16** in Figure 10. This indicates that the solution conformations of ferrocene peptides **20**–**28** are similar, although different from that of **16**. However, an important finding is that the helical chirality of Fca peptides is dominated only by the chirality of the N-terminal amino acid on Fca: Boc-Ala-Fca-Ala-OMe **20** displays a positive CD signal at about 480 nm that changes to negative in Boc-D-Ala-Fca-Ala-OMe **23** (Figure 11). On the other hand, the same change on the C terminus of Fca has no effect on the helicity of the central ferrocene core (**20**→**24**). The chirality of the outer Ala has no influence on the helical chiraliy of the ferrocene. In addition, a non-monotonous correlation between the magnitude of the CD signal and the number of Ala subunits was observed. Generally, the intensity of the CD signals increases as the length of the oligopeptides increases (**20** or **23**→**28**).

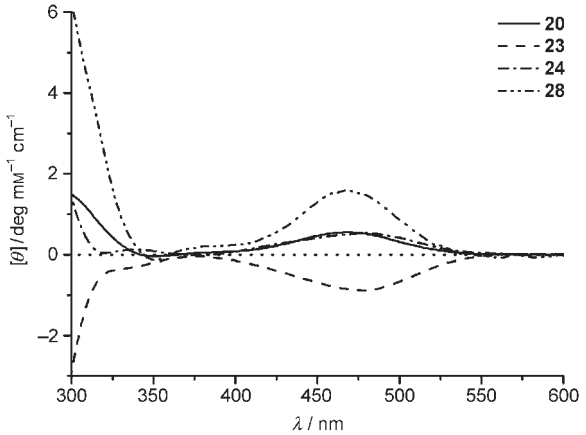

Figure 11. CD spectra (CH_3CN) of tripeptides **20**, **23**, and **24**, as well as pentapeptide **28**.

Notably, CD spectra give rise to relatively broad signals. Thus, signals arising from compounds that are structurally related, but slightly different, such as those studied here, will not be resolved. Also, dynamic equilibria are impossible to detect by CD spectroscopy alone.

NMR spectroscopy: ^{1}H NMR spectroscopy is a useful tool that enables us to describe the hydrogen bonding in our Fc peptides in solution in a more quantitative way. In general, the chemical shift of the amide protons should be higher in hydrogen-bonded structures than in the non-hydrogen-bonded state. However, because the equilibrium between

these states is too fast for the NMR timescale, we do not observe separate signals for these states. Rather, an average value for δ is observed at shifts higher than expected for the putative non-hydrogen-bonded species. To assign δ values to a specific conformer of a particular Fc peptide, we make use of reference compounds that cannot engage in hydrogen bonding, and that have NH groups in chemical environments similar to the Fca peptides with intramolecular hydrogen bonding. In general, it can be expected that an equilibrium between intramolecular hydrogen-bonded and non-hydrogen-bonded conformers is present in solution. The position of this equilibrium is strongly solvent dependent. Nonpolar aprotic solvents, such as $CHCl_3$ or CH_2Cl_2, favour intramolecular hydrogen-bonded structures, whereas polar solvents, such as DMSO, disrupt hydrogen bonding by competing with the hydrogen-bonding sites. For our studies, we compared NMR measurements in $[D_6]$DMSO to those taken in $CDCl_3$. The resulting chemical shift differences $\Delta\delta$ are used as a measure for the populations in the hydrogen-bonded and non-hydrogen-bonded states.[17]

As reference compounds, we chose simple Fc-carboxylic acid and Fc-amino derivatives FcCO-X (X = -NHMe (**2**), -Ala-OMe (**3**)) and Y-NHFc (Y = Ac- (**7**), Boc- (**8**), Boc-Ala- (**9**)), which are unable to engage in intramolecular hydrogen bonding. In $CDCl_3$, compounds **2**, **3**, and **7**–**9** exhibit chemical shifts of the amide protons at positions below δ of 7.00 ppm. In $[D_6]$DMSO, chemical shifts of $\delta > 7.00$ ppm for the amide protons are observed, indicative of intermolecular hydrogen bonding to the DMSO molecules.

If the $\Delta\delta$ of the NH proton of a putative hydrogen-bonded system is smaller than the $\Delta\delta$ of the reference compound, which is free of intramolecular hydrogen bonding, the system engages in intramolecular hydrogen bonding. The ratio of the $\Delta\delta$ values for the Fc peptide and its reference compound of each amide proton, the variation ratio (vr), is particularly useful for measuring the extent to which the amide proton is engaged in intramolecular hydrogen bonding (vr = $\Delta\delta$ of substrate/$\Delta\delta$ of reference).[17] Weak hydrogen bonds will have large values for vr. This is rationalized by the fact that DMSO will readily disrupt the intramolecular hydrogen bonding, causing a large $\Delta\delta$ for the amide proton, which is of the same magnitude as that for the non-hydrogen-bonded reference compound. Thus, vr values close to unity are expected. In the case of strong intramolecular hydrogen bonding, addition of DMSO will also cause disruption of the intramolecular hydrogen bond, however, the $\Delta\delta$ between $CHCl_3$ and DMSO will be significantly smaller than that of the reference compound, resulting in a vr value close to zero. This also addresses the position of the equilibrium between the hydrogen-bonded and non-bonded state. For vr values close to zero, the position of the equilibrium is shifted significantly towards the hydrogen-bonded state, whereas vr values close to unity indicate a shift to the non-hydrogen-bonded state (Table 2).

A good example to demonstrate this approach is dipeptide **16**. Figure 8 shows three potential intramolecular hydrogen-bonded conformers and one open conformer. In conformer **16A**, CO and NH groups attached directly to the Fc moiety are engaged in hydrogen bonding, resulting in a 6-membered ring. Conformer **16B** has a hydrogen bond between the amide Fc-CO-*NH* and the *CO*-NH-Fc, forming an 8-membered hydrogen-bonded ring. In conformer **16C**, the distal C=O group engages in hydrogen bonding with the NH-Fc group giving a 9-membered ring. In $CDCl_3$ solution, compound **16** exhibits two amide resonances: at $\delta =$ 6.77 ppm for the NH_{Ala} and at $\delta = 6.40$ ppm for the NH_{Fca} group. In $[D_6]$DMSO, the resonances at $\delta = 8.04$ ppm (NH_{Ala}) and 8.43 ppm (NH_{Fca}) are observed. The differences in chemical shift for the two amide protons in the two solvents are $\Delta\delta = 1.27$ ppm for the NH_{Ala} and $\Delta\delta = 2.03$ ppm

Table 2. Chemical shifts (δ), chemical shift differences ($\Delta\delta$), and variation ratios (vr) of the amide protons for selected compounds.

Compd	Formula	δ (CD_3Cl)[a]	δ ($[D_6]$DMSO)[a]	$\Delta\delta$	vr = $\Delta\delta$ substrate/ $\Delta\delta$ standard (standard)
2	Fc-CO-NH-Me[b]	5.73 (brs)	7.73 (d)	2.00	
3	Fc-CO-Ala-OMe	6.22 (brs)	8.07 (d)	1.85	
5	Fc-CO-Ala1-Ala2-OMe	6.27 (d), 6.86[c] (d)	7.71 (d), 8.28 (d)	1.44, 1.42	
7	Ac-NH-Fc	6.49 (brs)	9.28 (s)	2.79	
8	Boc-NH-Fc	5.55 (brs)	8.50 (s)	2.95	
9	Boc-Ala-NH-Fc	5.55 (brs), 6.83 (brs)	7.00 (d), 9.28 (s)	1.45, 2.45	
10	Boc-Ala2′-Ala1′-NH-Fc	5.09 (d), 6.78 (d), 8.04 (brs)	7.03 (d), 8.00 (d), 9.35 (s)	1.94, 1.22, 1.31	
12	Ac-Fca-NH-Me[c]	7.48 (brs), 6.23 (brs)	9.20 (s), 7.46 (d)	1.72, 1.23	0.62 (**7**), 0.61 (**2**)
15	Boc-Fca-NH-Me	5.88 (brs), 6.47 (brs)	8.42 (s), 7.62 (d)	2.54, 1.55	0.86 (**8**), 0.58 (**2**)
16	Boc-Fca-Ala-OMe	6.40 (s), 6.77 (s)	8.43 (brs), 8.04 (d)	2.03, 1.27	0.69 (**8**), 0.69 (**3**)
19	Boc-Fca-Ala1-Ala2-OMe	7.28 (brs), 7.01 (s), 6.90 (brs)	8.43 (brs), 7.71 (d), 8.29 (d)	1.15, 0.7, 1.39	0.39 (**8**), 0.49 (**5**), 0.98 (**5**)
20	Boc-Ala1′-Fca-Ala1-OMe	5.13 (d), 9.12 (s), 7.81 (d)	7.04 (d), 9.24 (s), 8.01 (d)	1.91, 0.12, 0.20	1.32 (**9**), 0.05 (**9**), 0.11 (**3**)
21	Boc-Ala1′-Fca-Ala1-Ala2-OMe	5.17 (d), 9.86 (brs), 7.96 (brs), 7.11 (d)	7.25 (d), 10.02 (s), 7.77 (d), 8.59 (d)	2.08, 0.16, −0.20, 1.48	1.43 (**9**), 0.07 (**9**), −0.14 (**5**), 1.04 (**5**)
22	Boc-Ala2′-Ala1′-Fca-Ala1-Ala2-OMe	5.28 (s), 7.20 (brs), 9.78 (brs), 8.06 (brs), 7.03 (brs)	7.00 (d), 8.12 (d), 9.61 (s), 7.87 (d), 8.53 (d)	1.72, 0.92, −0.17, −0.19, 1.50	1.19 (**9**), 0.75 (**10**), −0.07 (**9**), −0.13 (**5**), 1.05 (**5**)

[a] 5×10^{-3} to 2×10^{-4} M. [b] Fc ≡ ferrocenyl. [c] Fca ≡ 1′-aminoferrocene-1-carboxylic acid.

for the Fc-NH group. For each of the two amide protons it is important to choose an appropriate reference compound that has comparable amide groups, but cannot engage in intramolecular hydrogen bonding. The ideal reference compound for the NH-Fc amide in **16** is compound **8**. A good reference compound for the Ala_{NH} group is compound **3**, which has an Fc-CO-Ala-OMe. Both amides NH have the identical value for vr of 0.69, indicating the presence of medium-strength hydrogen bonds in compound **16**.

Tetrapeptide **21** is another good example to illustrate our approach. In $CDCl_3$, **21** displays four amide resonances at $\delta = 5.17$ ($NH_{Ala1'}$), 9.86 (NH_{Fca}), 7.96 (NH_{Ala1}), and 7.11 ppm (NH_{Ala2}). In [D_6]DMSO, the resonances shift to $\delta = 7.25$ ppm for $NH_{Ala1'}$, 10.02 ppm for NH_{Fca}, 7.77 ppm for NH_{Ala1}, and 8.59 ppm for NH_{Ala2}. The chemical shift of both proximal NH protons (NH_{Fca} and NH_{Ala1}) moves strongly downfield in $CDCl_3$ solutions if both Cp rings are substituted by amino acids, because of the formation of intramolecular hydrogen bonds that involve these two protons. This hydrogen bonding is disrupted in DMSO and as a consequence the order of the Ala1 and Ala2 amide protons is reversed. The chemical shift differences $\Delta\delta$ for the four amide resonances in **21** are 2.08, 0.16, −0.20, and 1.48 ppm. To evaluate the vr for the C-terminal Ala NH resonances we used reference compound **5**, whereas we choose reference compound **9** for the N-terminal side. For the presented order of amide resonances we obtained the following vr's: 1.43, 0.07, −0.14, 1.04. The vr values for the proximal NH groups of 0.07 and −0.14 indicate that the amides directly attached to the Fc group are engaged in strong intramolecular hydrogen bonding in $CDCl_3$.

IR spectroscopy: In the previous section it was emphasized that the conformational equilibrium between the specific intramolecular hydrogen-bonded and hydrogen-bond-free isomers is too fast on the NMR timescale to be detected as distinct NH signals. However, it is slow enough to be detected by IR spectroscopy and can be used as additional support for the existence of hydrogen-bonded and non-hydrogen-bonded isomers. In addition, IR spectroscopy allows us to approximate the population ratio of these two states from the relative intensities of the IR bands, which should be consistent with vr values[14] On the other hand, IR spectra are more difficult to assign in detail than ^{1}H NMR spectra. Therefore, we will use some of the simpler compounds as examples in the following discussion.

IR spectra of our compounds were recorded in dichloromethane solutions ($c = 10^{-2}$ M L^{-1}). In accordance with ^{1}H NMR data, reference compounds of the type Fc-COX (**2**, **3**) and YNH-Fc (**7**, **8**) showed only non-hydrogen-bonded NH signals in the amide A range of 3436–3465 cm^{-1}. The IR spectrum of dipeptide **5** with two Ala units exhibited NH stretching vibrations ν(NH) at 3426 and 3309 cm^{-1}. Upon dilution from 5 to 2.5 mM, the second band assigned to the hydrogen-bonded state gradually weakened and disappeared, indicating an intermolecular hydrogen-bonded species. In contrast, the IR spectra of YNH-Fc-types **9** and **10** displayed two amide A bands at 3425/3336 and 3423/3336 cm^{-1}, respectively, however, the intensity ratio of these absorption bands remained unchanged upon dilution, indicating that in compounds **9** and **10** medium-strength intramolecular hydrogen bonds involving the NH-Fc group are present. Again, this corresponds well to the NMR data presented in Table 2.

NMR data of peptide analogue **12** suggested a conformational equilibrium of two conformers **A** (6-membered hydrogen-bonded ring) and **B** (8-membered hydrogen-bonded ring), in analogy to dipeptide **16**. Okamura et al.[13b] performed IR analysis of this compound in dilute CH_2Cl_2 solution in comparison with the non-hydrogen-bonded reference compounds **2** and **7** and assigned the band at lower wavenumber to hydrogen-bonded amide NH. The absorption at higher wavenumber was assigned to non-hydrogen-bonded amide NH of the forms **A** and **B**. The intensity ratio of the two is close to unity, suggesting the presence of equal amounts of these two conformers.[13b] This finding is in accordance with the vr values of 0.61 and 0.62 that were derived for **12A** and **12B**.

We carried out a similar IR analysis of analogue **15** by using non-hydrogen-bonded compounds **2** and **8** as references. We observed two ν(NH) bands at 3460 and 3433 cm^{-1} (corresponding to bands at 3465 and 3436 cm^{-1} in **2** and **8**), which are assigned to free non-hydrogen-bonded amide protons of **B** and **A**, respectively. Instead of two distinct hydrogen-bonded NH absorptions as in compound **12**, we observed only a single broad absorption centered at 3357 cm^{-1}. However, the intensities of the free and hydrogen-bonded signals were approximately equal, corroborating our findings from NMR analysis of a medium-strength intramolecular hydrogen bond being present in peptide analogue **15**. The IR spectrum of compound **13** displays a single amide A band at 3433 m cm^{-1}, indicating a hydrogen-bond-free structure.

IR spectra of the dipeptides **16** and **17** show an amide A band typical of non-hydrogen-bonded NH at 3433 cm^{-1} and one hydrogen-bonded NH at 3327 cm^{-1}, of approximately equal intensity. This result supports those from our NMR measurements. Both NMR and IR analyses indicate that intramolecular hydrogen bonding in the tripeptide **19** is stronger than that of the related dipeptide **16**, because the IR band is slightly shifted to lower wavenumbers and its vr ratio is slightly higher than that found in compound **16**.

Our NMR analysis demonstrated that the higher peptides **20**–**22** belong to another structural type with very strong hydrogen bonds forming a 9-membered and an 11-membered ring. Expectedly, the IR spectra of these oligopeptides were very similar. They contained one relatively narrow band in the range 3426–3438 cm^{-1}, assigned to non-hydrogen-bonded NH and three broad signals at 3355–3373, 3283–3322, and 3251 cm^{-1} corresponding to intramolecular hydrogen bonding. The first absorption may be attributed to the weak or medium intramolecular hydrogen-bonded NH subunits of Ala1′, Ala2′, and Ala2. We assign the other absorptions to the strongly hydrogen-bonded NH_{Fca} group.

Electrochemistry: The electrochemical behavior of compounds **16**, **17**, and **23–28** was studied by cyclic voltammetry (CV). All ferrocene-containing amino-acid and peptide conjugates discussed in this study exhibit a reversible electrochemical one-electron oxidation. For Fca peptide derivatives, the half-wave potentials $E_{1/2}$ are observed within a range of 476–533 mV vs Ag/AgCl, with peak-to-peak separation ΔE_p of 63 to 98 mV, and with a Faradic current ratio of close to unity. Importantly, we do not observe any amino-acid- or peptide-specific trends. Such behavior has been noted before for ferrocene amino-acid conjugates.[5] All experimental values are listed in Table 3.

Table 3. Solution electrochemical results for compounds **16**, **17**, **23–28**.[a]

Compound	$E_{1/2}$	ΔE_p	I_a/I_c[b]
16	481	73	1.1
17	488	75	1.0
23	502	78	1.1
24	533	62	1.0
25	471	81	1.0
26	488	73	1.1
27	476	98	1.1
28	483	74	1.1

[a] Conditions: 1 mM in MeCN; glassy carbon working electrode (BAS), Pt counter, Ag/AgCl reference, 0.1 M TBAP; E in mV; errors in the measured potentials are ± 5 mV from five independent measurements. [b] I_a/I_c = ratio of anodic to cathodic peak current.

Conclusions

Fca is one of the simplest organometallic amino acids based on the ferrocene skeleton. We have provided a synthetic approach to amino-acid and peptide conjugates of Fca, giving the desired compounds in good to excellent yields. We used standard peptide-coupling techniques and two different synthesis strategies: The first strategy uses attachment of amino acids or dipeptides directly to either the C or N terminus of Fca. The second strategy includes coupling of one amino acid to Fca, its deprotection, and subsequent coupling of the second amino acid. This second strategy can also be applied to both Fca termini.

By using this synthetic approach, di- to pentapeptides containing Fca as an organometallic amino acid were obtained by peptide chemistry in solution. Depending on the substitution pattern, these compounds exhibit turn-like peptide structures that are stable in solution and in the solid state. Characterization of the hydrogen-bonding patterns in solution is particularly challenging and we have used a combination of various spectroscopic techniques to obtain detailed information about solution conformations. To distinguish between possible conformers we used a nomenclature that indicates the relative orientation of the amide groups directly bound to the ferrocene core (Figures 7 and 8). A more detailed description of a general nomenclature for metallocene-based peptides has been proposed recently.[5b]

The X-ray structures of dipeptides **16–18** and the tetrapeptide **21** have been obtained and were examined in detail. The dipeptides show a conformer **B** in the solid state, with one intramolecular interstrand hydrogen bond. In contrast, conformer **C** with two intramolecular hydrogen bonds is found in the crystal of the tetrapeptide **21**.

Helical chirality of the metallocene core, a very important property of the Fca peptides, was studied by X-ray crystallography and CD spectroscopy. The representative examples **16** and **21** differ not only in their hydrogen-bonding pattern (see previous paragraph), but also in helical chirality. Dipeptide **16** was found to be in the *M*,L stereochemistry in the solid state. The CD spectrum of **16** shows a negative band at about 500 nm. For **21**, however, the crystal structure reveals an L,*P*,L,L stereochemistry and the CD spectrum shows a positive signal at about 480 nm. CD spectroscopy has been used previously to elucidate the metal-centered chirality in peptide derivatives of ferrocene-1,1′-dicarboxylic acid.[5b,7b] Hirao and co-workers showed that peptides made from hydrogen bonding L-amino acids on both Cp rings induces *P* chirality of the metallocene core. In a recent paper, one of our groups could show that equilibrium mixtures of *M* and *P* helicity exist if amino acids of *different* chirality are attached to either ring in such systems.[9c] For Fca peptides, the situation is different again, as shown herein. Metallocene chirality is purely dependent on the chirality of the first amino acid attached to the Fca amino group.

^{1}H NMR spectra were used to further elucidate the hydrogen-bonding pattern. Monosubstituted Fc derivatives were used as reference points of non-hydrogen bonded structures. The variation ratio vr was established, which reflects the ability of the Fca-peptide conjugates to engage in hydrogen bonding and, thus, provides information regarding the hydrogen-bond strength in the peptide conjugates. A vr value close to zero is indicative for strong hydrogen bonding. It is no surprise that the ability to maintain a conformation is linked to the length of the peptide chain. Thus, short Fca peptides, such as **16–18**, are unable to establish more than one single hydrogen bond in solution. As a consequence, they exist as a mixture of conformers in solution. The longer Fca-peptides **20–28** can form two intramolecular hydrogen bonds between the pendant peptide chains, resulting in a single conformer in the solid state as well as in solution.

Results of IR spectroscopy generally confirm the findings from NMR spectroscopy. However, IR spectroscopy operates on a faster time scale than NMR spectroscopy. Hence, signals for free protons ($>3400\ cm^{-1}$, sharp signals) and hydrogen-bonded amide protons ($<3400\ cm^{-1}$ and broader) are clearly resolved. Integration of the amide IR signals gives the ratio of free and hydrogen-bonded species directly. This ratio correlates well with the parameter vr as defined for ^{1}H NMR spectroscopy for all systems investigated in this study.

A number of organometallic amino acids have been synthesized previously, such as ferrocenylalanine and (ferrocene-1,1′-diyl)bisalanine.[5a] Some of those compounds were incorporated into peptides, mostly by solution chemistry.[18] The peptides described herein differ from these systems in that each Cp ring of the metallocene backbone is connected

directly to either the amino or carboxylic acid. The energetic barrier for rotation of the two Cp rings is small. This provides a degree of flexibility to such systems that is not achievable with the more-common organic peptide mimetics. Janda and co-workers made use of this low rotational barrier in disubstituted ferrocenes to generate catalytic antibodies for *endo*- and *exo*-stereoselective Diels–Alder reactions from one single ferrocene hapten.[12] Therefore, oligopeptides derived from Fca possess special properties and may form unique secondary and tertiary structures. The systematic work described herein lays a solid foundation for the rational design of such unique metallocene peptides.

Experimental Section

Most of the syntheses were carried out under argon. The CH_2Cl_2 used for synthesis and FTIR was dried (P_2O_5), distilled over CaH_2, and stored over molecular sieves (4 Å). EDC, HOBt, HBTU (Aldrich), and Ala (Merck) were used as received. Products were purified by preparative thin layer chromatography (TLC) on silica gel (Merck, Kieselgel 60 HF_{254}) by using the mixtures CH_2Cl_2/EtOAc and CH_2Cl_2/MeOH. Melting points were determined by using a Buechi apparatus. Infrared spectra were recorded as CH_2Cl_2 solutions between NaCl windows or as KBr disks by using a Bomem MB 100 mid FTIR, a Bruker Equinox55 FTIR, or a Perkin–Elmer model 1605 FTIR spectrometer. The ^{1}H and ^{13}C NMR spectra were recorded in $CDCl_3$ and [D$_6$]DMSO solutions with Me_4Si as internal standard by using a Varian EM 360, Varian Gemini 300 spectrometer. NMR spectra were determined by using a Bruker AM 360 spectrometer, ^{1}H at 360.14 MHz and ^{13}C at 90.56 MHz. High field 1D- and 2D-NMR spectra were recorded by using Bruker DRX 500 or Bruker Avance-500 spectrometers, ^{1}H at 500.13 MHz. Spectral assignment for peptide oligomers was carried out by using standard 2D-NMR spectroscopy. Peak positions are reported in ppm relative to TMS and are referenced by using the residual undeuterated solvent signal. UV/Vis spectra were measured by using a Varian CARY 100 instrument in 1-cm quartz Suprasil cells thermostated at 20 °C. Absorption maxima, λ_{max}, and molar absorption coefficients, ε_{max}, are given in nm and $M^{-1}cm^{-1}$, respectively. Mass spectra (MS) were run on MAT 8200 (EI, FAB) or Hewelett–Packard HP 5989 (ESI). Only characteristic fragments with possible composition are given in brackets. For fragments containing metals, only the isotopomer with highest intensity was described. Crystallographic analyses were performed by using a Bruker SMART-CCD difractometer. CD spectra were recorded as CH_3CN solutions ($c = 1$ M) by using a CD-spectropolarimeter Jasco-810 in 1-cm quartz Suprasil cells under inert atmosphere thermostated at 20 °C. Ellipticity maxima, λ_{max}, are given in nm. Molar ellipticity coefficients, $[\theta]$, were calculated as $[\theta] = 100 \times \theta / c \times l$, in which ellipticity $[\theta]$ is in degrees, concentration c is in mol L^{-1} and pathlength l is in cm, to give units for $[\theta]$ of deg mM^{-1}cm^{-1}.[19] Elemental analyses were determined in-house. The numbering of Ala subunits is presented in Table 2.

Synthesis of *N*-methylferrocenecarboxamide (2): EDC (367 mg, 1.91 mmol) and HOBt (266 mg, 1.91 mmol) were added to a suspension of ferrocenecarboxylic acid **1** (400 mg, 1.74 mmol) in dichloromethane (7 mL). After stirring for 1 h at RT, the mixture was cooled to 0 °C and CH_3NH_2 (3.48 mmol) (obtained from CH_3NH_2·HCl by treatment with Et_3N in CH_2Cl_2, pH ~ 8) was added. The mixture was stirred for 1 h at RT, washed thrice with saturated solution of $NaHCO_3$, 10 % aqueous solution of citric acid, and H_2O, then dried over Na_2SO_4, and evaporated in vacuo. TLC purification of crude product with CH_2Cl_2/EtOAc (5:1) gave orange crystals (321 mg, 76 %). M.p 178.1–179 °C;[13b] ^{1}H NMR ([D$_6$]DMSO): $\delta = 7.73$ (d, $J = 3.7$ Hz 1H; NH), 4.75 (s, 2H; H-2, H-5, Fc), 4.32 (s, 2H; H-3, H-4, Fc), 4.15 (s, 5H; Cp$_{unsubst.}$), 2.70 ppm (d, $J = 4.5$ Hz, 3H; CH_3); ^{1}H NMR ($CDCl_3$): $\delta = 5.73$ (brs, 1H; NH), 4.66 (brs, 2H; H-2, H-5, Fc), 4.36 (s, 2H; H-3, H-4, Fc), 4.22 (s, 5H; Cp$_{unsubst.}$), 3.02 ppm (brs, 3H; CH_3); ^{13}C NMR ([D$_6$]DMSO): $\delta = 168.7$ (CO), 76.4 (C-1, Fc), 69.1 (C-2 C-5, Fc), 68.7 (Cp$_{unsubst.}$), 67.5 (C-3 C-4, Fc), 25.3 ppm (CH_3); IR (CH_2Cl_2): $\tilde{\nu} = 3465$ (m, N-H free), 1657 cm^{-1} (s, C=O).

Synthesis of Fc-CO-Ala-OMe (3): Ferrocenecarboxylic acid **1** (300 mg, 1.30 mmol) was activated by using standard EDC/HOBt method. After stirring for 1 h at RT, the mixture was cooled to 0 °C and Ala-OMe (2.61 mmol) (obtained from H-Ala-OMe·HCl by treatment with Et_3N in CH_2Cl_2, pH ~ 8) was added. The reaction mixture was stirred for 1 h at RT, and worked-up as described for compound **2**. TLC purification of crude product with CH_2Cl_2/EtOAc (10:1) gave orange crystals (352 mg, 85 %). M.p 162–165 °C;[20] ^{1}H NMR ([D$_6$]DMSO): $\delta = 8.07$ (d, $J = 7.11$ Hz, 1H; NH), 4.90 (s, 1H; H-5, Fc), 4.79 (s, 1H; H-2, Fc), 4.44–4.32 (m, 3H; CH_{Ala}, H-3, H-4, Fc), 4.22 (s, 5H; Cp$_{unsubst.}$), 3.60 (s, 3H; OCH_3), 1.37 ppm (d, $J = 7.3$ Hz, 3H; CH_{3Ala}); ^{1}H NMR ($CDCl_3$): $\delta = 6.22$ (brs, 1H; NH), 4.76 (brs, 2H; H-2, H-5, Fc), 4.68 (s, 1H; CH_{Ala}), 4.38 (s, 2H; H-3, H-4, Fc), 4.26 (s, 5H; Cp$_{unsubst.}$), 3.80 (s, 3H; OCH_3), 1.49 ppm (d, $J = 5.7$ Hz, 3H; CH_{3Ala}); ^{13}C NMR ([D$_6$]DMSO): $\delta = 173.6$ (COFc), 169.2 (*C*OOCH), 75.7 (C-1, Fc), 70.3 (C-2, Fc), 70.3 (C-5, Fc), 69.6 (Cp$_{unsubst.}$), 68.7 (C-3, Fc), 68.3 (C-4, Fc), 52.0 (OCH_3), 47.8 (CH_{Ala}), 17.1 ppm (CH_{3Ala}); IR (CH_2Cl_2): $\tilde{\nu} = 3436$ (m, N-H free), 1741 (s, C=O, $COOCH_3$), 1657 cm^{-1} (s, C=O, CONH).

Synthesis of Fc-CO-Ala-Ala-OMe (5): Hydrolysis of peptide **3** (100 mg, 0.32 mmol) in dioxane/water (1:1) mixture (10 mL) at 0 °C in the presence of NaOH (25 mg, 0.64 mmol) resulted in the formation of the free acid Fc-CO-Ala-OH (**4**). Compound **4** was isolated in 95 % yield by acidification of the solution with 2 % HCl to pH 2, followed by extraction with EtOAc (3 × 30 mL). The organic layer was dried over anhydrous Na_2SO_4, filtered, and the solvent was removed under reduced pressure to give an orange residue. IR (CH_2Cl_2): $\tilde{\nu} = 3433$ (m, N-H free), 3100–2900 (br, OH, COOH), 1731 (s, C=O, COOH), 1655 cm^{-1} (s, CONH).

The free acid **4** (96 mg, 0.32 mmol) was reacted with Ala-OMe (0.63 mmol) (obtained from Ala-OMe·HCl by treatment with Et_3N in CH_2Cl_2, pH ~ 8), EDC (67 mg, 0.35 mmol), and HOBt (49 mg, 0.35 mmol) in dichloromethane. After stirring for 90 min at RT, the reaction mixture was subjected to the aqueous work-up described above for **2**. TLC purification of crude product with CH_2Cl_2/EtOAc (10:1) gave a yellow solid (60 mg, 50 %). M.p 122–125 °C (124–126 °C[20]); ^{1}H NMR ([D$_6$]DMSO): $\delta = 8.28$ (d, $J = 6.8$ Hz, 1H; NH_{Ala2}), 7.71 (d, $J = 7.7$ Hz, 1H; NH_{Ala1}), 4.90 (s, 1H; H-5, Fc), 4.79 (s, 1H; H-2, Fc), 4.46 (m, 1H; CH_{Ala2}), 4.43 (m, 3H; CH_{Ala1}, H-3, H-4, Fc), 4.18 (s, 5H; Cp$_{unsubst.}$), 3.62 (s, 3H; OCH_3), 1.32 (d, $J = 1.2$ Hz, 3H; CH_{3Ala2}) 1.30 ppm (d, $J = 1.9$ Hz, 3H; CH_{3Ala1}); ^{1}H NMR ($CDCl_3$): $\delta = 6.86$ (d, 1H; NH_{Ala2}), 6.27 (d, 1H; NH_{Ala1}), 4.82 (m, 1H; CH_{Ala2}), 4.75 (s, 2H; H-2, H-5, Fc), 4.55 (m, 1H; CH_{Ala1}), 4.35 (s, 2H; H-3, H-4, Fc), 4.20 (s, 5H; Cp$_{unsubst.}$), 3.75 (s, 3H; OCH_3), 1.50 (d, $J = 6.8$ Hz, 3H; CH_{3Ala2}) 1.44 ppm (d, $J = 7.1$ Hz, 3H; CH_{3Ala1}); ^{13}C NMR ([D$_6$]DMSO): $\delta = 172.6$ (COFc), 172.1 (CO_{Ala1}), 169.9 (*CO*OCH_3), 74.8 (C-1, Fc), 70.2 (C-2 C-5, Fc), 69.7 (Cp$_{unsubst.}$), 68.0 (C-3 C-4, Fc), 51.9 (OCH_3), 48.1 (CH_{Ala2}), 48.0 (CH_{Ala1}), 18.3 (CH_{3Ala2}), 17.3 ppm (CH_{3Ala1}); IR (CH_2Cl_2): $\tilde{\nu} = 3426$ (m, N-H free), 3309 (w, N-H assoc.), 1742 (s, C=O, $COOCH_3$), 1682 (s), 1650 cm^{-1} (s, C=O, CONH).

Synthesis of ferrocenecarboxazide (6): Ferrocenecarboxylic acid **1** (400 mg, 1.74 mmol) was suspended in water (0.3 mL) and sufficient acetone was added to dissolve it. After cooling to 0 °C, triethylamine (202 mg, 2.0 mmol) in acetone (3.3 mL) was added. While maintaining the temperature at 0 °C, a solution of ethyl chloroformate (241.6 mg, 2.23 mmol) in the same solvent (0.9 mL) was added and the mixture was stirred for 30 min at 0 °C. Thereafter, a solution of sodium azide (173 mg, 2.63 mmol) in water (0.5 mL) was added. The mixture was stirred for 1 h (0 °C), poured into excess of ice water, and extracted with dichloromethane. The extracts were washed with 5 % aqueous solution of $NaHCO_3$, a saturated solution of NaCl, dried over Na_2SO_4, and evaporated in vacuo at RT to dryness to leave red crystals (332 mg, 75 %). M.p. 101–102 °C; ^{1}H NMR ($CDCl_3$): $\delta = 4.83$ (s, 2H; H-2, H-5, Fc), 4.52 (s, 2H; H-3, H-4, Fc), 4.27 ppm (s, 5H; Cp$_{unsubst.}$); IR (CH_2Cl_2): $\tilde{\nu} = 2138$ (s, N_3), 1687 cm^{-1} (s, C=O, CON_3).

Synthesis of *N*-acetylferrocenamine (7): A solution of ferrocenecarboxazide (**6**) (332 mg, 1.3 mmol) in acetic anhydride (9 mL) was heated at 100 °C for 3 h.[11a] After cooling, the reaction mixture was diluted with

water (40 mL) and extracted with dichloromethane. After aqueous work-up, the organic layer was evaporated to dryness giving a red oil, which after TLC purification with dichloromethane/ethyl acetate (10:1) gave orange crystals (78 mg, 25%). M.p. 158–167°C;[13b] ^{1}H NMR ([D$_6$]DMSO): δ=9.28 (s, 1H; NH), 4.54 (s, 2H; H-2, H-5, Fc), 4.10 (s, 5H; Cp$_{unsubst.}$), 3.93 (s, 2H; H-3, H-4, Fc), 1.90 ppm (s, 3H; CH$_3$); ^{1}H NMR ($CDCl_3$): δ=6.49 (brs, 1H; NH), 4.93 (brs, 2H; H-2, H-5, Fc), 4.36 (s, 5H; Cp$_{unsubst.}$), 4.22 (s, 2H; H-3, H-4, Fc), 1.99 ppm (s, 3H; CH$_3$); ^{13}C NMR ([D$_6$]DMSO): δ=168.0 (*C*OCH$_3$), 95.7 (C-1′, Fc), 68.9 (Cp$_{unsubst.}$), 63.8 (C-3′ C-4′, Fc), 60.8 (C-2′ C-5′, Fc), 23.6 ppm (CH$_3$); IR (CH_2Cl_2): $\tilde{\nu}$=3436 (m, N-H free), 1684 cm^{-1} (s, C=O, COCH$_3$).

Synthesis of *tert*-butyl ferrocenylcarbamate (8): A solution of ferrocenecarboxazide **6** (400 mg, 1.6 mmol) in *t*BuOH (10 mL) was heated at 60°C for 2 h.[14a] The reaction mixture was evaporated to dryness and purified by preparative chromatography in dichloromethane/ethyl acetate (25:1), giving orange crystals of **8** (320 mg, 68%), m.p. 142–145°C and *N*,*N*′-diferrocenylurea (60 mg, 9%), m.p. 167–173°C. ^{1}H NMR ([D$_6$]DMSO): δ= 8.50 (brs, 1H; NH), 4.44 (s, 2H; H-2′, H-5′, Fc), 4.08 (s, 5H; Cp$_{unsubst.}$), 3.89 (s, 2H; H-3′, H-4′, Fc), 1.45 ppm (s, 9H; C(C*H*$_3$)$_3$); ^{1}H NMR ($CDCl_3$): δ=5.55 (brs, 1H; NH), 4.60 (brs, 2H; H-2′, H-5′, Fc), 4.24 (s, 5H; Cp$_{unsubst.}$), 4.11 (brs, 2H; H-3′, H-4′, Fc), 1.50 ppm (s, 9H; C(C*H*$_3$)$_3$); IR (CH_2Cl_2): $\tilde{\nu}$=3436 (m, N-H free), 1723 cm^{-1} (s, C=O, COO*t*Bu).

Synthesis of Boc-Ala-NH-Fc (9): A suspension of **8** (500 mg, 1.66 mmol) in ethyl acetate (20 mL) was cooled to 0°C and treated with gaseous HCl for 2 h. After stirring at RT for 4 h, mixture was evaporated in vacuo to dryness to leave yellow solid ferrocenylammonium chloride (370 mg, 94%). The hydrochloride (238 mg, 1.06 mmol) was treated with Et_3N in CH_2Cl_2 (pH ~8) and coupled with Boc-Ala-OH (189 mg, 2.11 mmol) by using the standard EDC/HOBt method. After stirring for 1 h at RT, the mixture was subjected to the standard aqueous work-up, followed by TLC purification (CH_2Cl_2/EtOAc, 10:1) to give yellow crystals (232 mg, 60%). M.p. 68–70°C; ^{1}H NMR ([D$_6$]DMSO): δ=9.28 (s, 1H; FcNH), 7.00 (d, J=6.8 Hz, 1H; NH$_{Ala}$), 4.61 (s, 2H; H-2′, H-5′, Fc), 4.09 (s, 5H; Cp$_{unsubst.}$), 3.93 (s, 3H; CH$_{Ala}$, H-3′, H-4′, Fc), 1.39 (s, 9H; C(C*H*$_3$)$_3$), 1.20 ppm (d, J=7.08 Hz, 3H; CH$_{3Ala}$); ^{1}H NMR ($CDCl_3$): δ=6.83 (brs, 1H; FcNH), 5.55 (brs, 1H; NH$_{Ala}$), 5.20–4.10 (m, 9H; Fc-H), 3.95 (brs, 1H; CH$_{Ala}$), 1.47 (s, 9H; C(C*H*$_3$)$_3$), 1.28 ppm (d, J=6.2 Hz, 3H; CH$_{3Ala}$); ^{13}C NMR ([D$_6$]DMSO): δ=171.5 (CO$_{Ala}$), 155.3 (COO*t*Bu), 95.6 (C-1′, Fc), 78.2 (*C*(CH$_3$)$_3$), 68.9 (Cp$_{unsubst.}$), 63.9 (C-3′, Fc), 63.8 (C-4′, Fc), 60.9 (C-2′, Fc), 60.6 (C-5′, Fc), 50.4 (CH$_{Ala}$), 28.4 (C(*C*H$_3$)$_3$), 18.0 ppm (CH$_{3Ala}$); IR (CH_2Cl_2): $\tilde{\nu}$=3425 (m, N-H free), 3336 (vw, N-H assoc.), 1697 cm^{-1} (s, C=O, COO*t*Bu).

Synthesis of Boc-Ala-Ala-NH-Fc (10): Boc-Ala-NH-Fc (**9**) (362 mg, 0.41 mmol) was deprotected by treating with gaseous HCl. The resulting Ala-NH-Fc·HCl was worked-up with Et_3N as described previously and coupled with Boc-Ala-OH (157 mg, 0.83 mmol) activated with HOBt/EDC. The mixture was stirred for 90 min at RT and worked-up in a usual manner. Purification by TLC (CH_2Cl_2/EtOAc, 10:1) gave yellow crystals (172 mg, 94%). M.p. 172–175°C; ^{1}H NMR ([D$_6$]DMSO): δ=9.35 (s, 1H; FcNH), 8.00 (d, J=6.9 Hz, 1H; NH$_{Ala1}$), 7.03 (d, J=6.8 Hz, 1H; NH$_{Ala2}$), 4.60 (d, J=4.5 Hz, 2H; H-2′, H-5′, Fc), 4.25 (m, 1H; CH$_{Ala2}$), 4.08 (s, 5H; Cp$_{unsubst.}$), 3.95 (m, 3H; CH$_{Ala1}$, H-3′, H-4′, Fc), 1.39 (s, 9H; C(C*H*$_3$)$_3$), 1.26 (d, J=7.0 Hz, 3H; CH$_{3Ala2}$), 1.19 ppm (d, J=6.9 Hz, 3H; CH$_{3Ala1}$); ^{1}H NMR ($CDCl_3$): δ=8.04 (brs, 1H; FcNH), 6.78 (brs, 1H; NH$_{Ala1}$), 5.09 (d, J=5.3 Hz, 1H; NH$_{Ala2}$), 4.81 (brs, 1H; H-2′, Fc), 4.67 (brs, J=4.5 Hz, 1H; H-5′, Fc), 4.48 (m, 1H; CH$_{Ala2}$), 4.19 (s, 6H; Cp$_{unsubst.}$, CH$_{Ala1}$), 4.05 (brs, 2H; H-3′, H-4′, Fc), 1.48 (s, 9H; C(C*H*$_3$)$_3$), 1.42 ppm (m, 6H; CH$_{3Ala2}$, CH$_{3Ala1}$); ^{13}C NMR ([D$_6$]DMSO): δ=172.0 (CO$_{Ala2}$), 170.2 (CO$_{Ala1}$) 154.73 (COO*t*Bu), 94.7 (C-1′, Fc), 77.6 (*C*(CH$_3$)$_3$), 68.3 (Cp$_{unsubst.}$), 63.3 (C-3′ C-4′, Fc), 60.3 (C-2′, Fc), 60.0 (C-5′, Fc), 49.3 (CH$_{Ala2}$), 48.2 (CH$_{Ala1}$), 27.7 (C(*C*H$_3$)$_3$), 17.7 (CH$_{3Ala2}$), 17.5 ppm (CH$_{3Ala1}$); IR (CH_2Cl_2): $\tilde{\nu}$=3423 (m, N-H free), 3336 (m, N-H assoc.), 1698 cm^{-1} (s, C=O, COO*t*Bu).

Synthesis of Ac-Fca-NHMe (12): Ac-Fca (**11**)[14a] (230 mg, 0.80 mmol) was activated as described for **1** and $MeNH_2$ (obtained from $MeNH_2$·HCl (108 mg, 1.60 mmol) by treatment with Et_3N in CH_2Cl_2, pH ~8) was added. After stirring for 1 h at RT, the reaction mixture was worked-up in a usual manner and purified by TLC (CH_2Cl_2/EtOAc, 10:1) to give orange crystals (81 mg, 43%). M.p. 128–130°C;[15][1] ^{1}H NMR ([D$_6$]DMSO): δ=9.20 (s, 1H; NH$_{Fca}$), 7.46 (d, J=3.8 Hz, 1H; N*H*CH$_3$), 4.69 (s, 2H; H-2, H-5, Fc), 4.54 (s, 2H; H-2′, H-5′, Fc), 4.24 (s, 2H; H-3, H-4, Fc), 3.91 (s, 2H; H-3′, H-4′, Fc), 2.68 (d, J=4.4 Hz, 3H; NHC*H*$_3$), 1.90 ppm (s, 3H; COCH$_3$); ^{1}H NMR ($CDCl_3$): δ=7.48 (brs, 1H; NH$_{Fca}$), 6.23 (brs, 1H; N*H*CH$_3$), 4.63 (brs, 2H; H-2, H-5, Fc), 4.52 (brs, 2H; H-2′, H-5′, Fc), 4.36 (s, 2H; H-3, H-4, Fc), 4.09 (s, 2H; H-3′, H-4′, Fc), 2.94 (s, 3H; NHC*H*$_3$), 2.10 ppm (s, 3H; COCH$_3$); IR (CH_2Cl_2): $\tilde{\nu}$=3459 (m, N-H free), 3431 (m, N-H free), 3339 (w, N-H assoc.), 3272 (w, N-H assoc), 1680 cm^{-1} (s, C=O, COCH$_3$).

Synthesis of Boc-Fca-NHMe (15): Amide-carbamate **15** was prepared starting from $MeNH_2$ (obtained by the action of Et_3N on $MeNH_2$·HCl (117 mg, 1.74 mmol)) and **14** (activated with HOBt (182 mg, 1.30 mmol) and EDC (250 mg, 1.30 mmol)) in dichloromethane. The mixture was stirred for 30 min at RT. After the aqueous work-up, the crude product was purified by TLC (CH_2Cl_2/EtOAc, 5:1) to give orange crystals (283 mg, 91%). M.p. 128–130°C; ^{1}H NMR ([D$_6$]DMSO): δ=8.42 (s, 1H; NH$_{Fca}$), 7.62 (d, J=4.5 Hz, 1H; N*H*CH$_3$), 4.66 (s, 2H; H-2, H-5, Fc), 4.43 (s, 2H; H-2′, H-5′, Fc), 4.21 (s, 2H; H-3, H-4, Fc), 3.86 (s, 2H; H-3′, H-4′, Fc), 2.68 (d, J=4.5 Hz, 3H; NHC*H*$_3$), 1.45 ppm (s, 9H; C(C*H*$_3$)); ^{1}H NMR ($CDCl_3$): δ=6.47 (brs, 1H; N*H*CH$_3$), 5.88 (brs, 1H; NH$_{Fca}$), 4.71–4.23 (m, 8H; Fn), 3.09 (s, 3H; NHC*H*$_3$), 1.49 ppm (s, 9H; C(C*H*$_3$)); IR (CH_2Cl_2): $\tilde{\nu}$=3460 (m, N-H, FcNHCO free), 3433 (m, N-H, FcCONH free), 3367 (w, N-H, FcNHCO assoc.), 3357 (w, N-H, FcNHCO assoc.), 1680 cm^{-1} (s, C=O, COCH$_3$).

General synthesis of the ferrocene dipeptides 16–18: 1′-(*tert*-Butoxycarbonyl-amino)ferrocene-1-carboxylate (**14**, Boc-Fca-OH) (200 mg, 0.58 mmol) was activated by using EDC (167 mg, 0.87 mmol) and HOBt (117 mg, 0.87 mmol), and H-Aaa-OMe (1.16 mmol, obtained from H-Aaa-OMe·HCl by treatment with Et_3N in CH_2Cl_2, pH ~8) was added. The mixture was stirred for 30 min. After the standard aqueous work-up, the crude products were purified by TLC (CH_2Cl_2/EtOAc, 10:1) to give orange crystalline materials after standing in the refrigerator.

Boc-Fca-Ala-OMe (16): Orange powder (182 mg, 74%). M.p. 61–64°C; ^{1}H NMR ([D$_6$]DMSO): δ=8.43 (brs, 1H; NH$_{Fca}$), 8.04 (d, J=5.6 Hz, 1H; NH$_{Ala}$), 4.75 (s, 1H; H-2, Fn), 4.70 (s, 1H; H-5, Fn), 4.49 (m, 1H; CH$_{Ala}$), 4.40 (m, 2H; H-2′, H-5′, Fn), 4.25 (s, 2H; H-3, H-4, Fn), 3.92 (m, 2H; H-3′, H-4′, Fn), 3.64 (s, 3H; OCH$_3$), 1.45 (s, 9H; C(CH$_3$)$_3$), 1.38 ppm (d, J= 7.2 Hz, 3H; CH$_{3Ala}$); ^{1}H NMR ($CDCl_3$): δ=6.77 (s, 1H; NH$_{Ala}$), 6.40 (NH$_{Fca}$), 4.79 (brs, 1H; CH$_{Ala}$), 4.68–4.00 (m, 8H; Fc-H), 3.79 (s, 3H; OCH$_3$), 1.49 ppm (brs, 12H; C(CH$_3$)$_3$, CH$_{3Ala}$); ^{13}C NMR ([D$_6$]DMSO): δ=173.4 (*C*OOCH$_3$), 168.9 (CO$_{Fca}$), 153.1 (COO*t*Bu), 98.0 (C-1′, Fn), 78.7 (*C*(CH$_3$)$_3$), 75.6 (C-1, Fn), 71.3 (C-2 C-5, Fn), 68.9 (C-3′ C-4′, Fn), 65.4 (C-3 C-4, Fn), 61.1 (C-2′ C-5′, Fn), 51.7 (OCH$_3$), 47.7 (CH$_{Ala}$), 28.04 (C(*C*H$_3$)$_3$), 16.8 ppm (CH$_{3Ala}$); IR (CH_2Cl_2): $\tilde{\nu}$=3433 (m, N-H free), 3327 (m, N-H assoc.), 1731 (s, C=O, COOCH$_3$), 1714 (s, C=O, COO*t*Bu), 1655 cm^{-1} (s, C=O, CONH); EIMS: *m*/*z*: 430 (17) [*M*]$^+$, 374 (16) [*M*−H$_2$CC(CH$_3$)$_2$]$^+$, 356 (32) [*M*−*t*BuOH]$^+$, 330 (86) [H$_2$NCpFeCpCOAlaOMe]$^+$, 300 (19) [*M*−COAlaOMe]$^+$, 130 (35) [COAlaOMe]$^+$, 57 (100); ESI-MS (MeOH): *m*/*z*: 883.4 [2*M*+Na]$^+$; elemental analysis calcd (%) for $C_{20}H_{26}O_5N_2Fe$ (430.1): C 55.84, H 6.09, N 6.51; found: C 55.89, H 6.11, N 6.53.

Boc-Fca-D-Ala-OMe (17): Orange powder (183 mg, 75%). M.p. 61–63°C; IR (CH_2Cl_2): $\tilde{\nu}$=3433 (m, N-H free), 3327 (m, N-H assoc.), 1731 (s, C=O, COOCH$_3$), 1716 (s, C=O, COO*t*Bu), 1655 cm^{-1} (s, C=O, CONH); elemental analysis calcd (%) for $C_{20}H_{26}O_5N_2Fe$ (430.1): C 55.84, H 6.09, N 6.51; found: C 55.87, H 6.07, N 6.54.

Boc-Fca-β-Ala-OMe (18): Orange powder (178 mg, 79%). M.p. 61–64°C; ^{1}H NMR ([D$_6$]DMSO): δ=8.41 (brs, 1H; NH$_{Fca}$), 7.80 (t, 1H; NH$_{Ala}$), 4.67 (d, 2H; H-2, H-5, Fn), 4.42 (s, 2H; H-2′, H-5′, Fn), 4.22 (s, 2H; H-3, H-4, Fn), 3.86 (s, 2H; H-3′, H-4′, Fn), 3.62 (s, 3H; OCH$_3$), 3.33 (s, 4H; (CH$_2$)$_2$), 1.45 ppm (s, 9H; C(CH$_3$)$_3$); IR (CH_2Cl_2): $\tilde{\nu}$=3436 (m, N-H free), 3341 (w, N-H assoc.), 1728 (s, C=O, COOCH$_3$), 1712 (s, C=O, COO*t*Bu), 1653 cm^{-1} (s, C=O, CONH); elemental analysis calcd (%) for $C_{20}H_{26}O_5N_2Fe$ (430.1): C 55.84, H 6.09, N 6.51; found: C 55.82, H 6.06, N 6.54.

Synthesis of Boc-Fca-Ala-Ala-OMe (19): Boc-Fca-OH (**14**) (360 mg, 1.05 mmol) was activated as described for dipeptides **16–18** and coupled

with H-Ala-Ala-OMe (obtained from H-Ala-Ala-OMe·HCl by treatment with Et_3N in CH_2Cl_2). The mixture was stirred for 4 h at RT. After an aqueous work-up, the crude material was purified by TLC (CH_2Cl_2/EtOAc, 10:1) to give an orange crystalline solid (420 mg, 76%). M.p. 186.8–189.1 °C; ^{1}H NMR ([D$_6$]DMSO): δ = 8.43 (s, 1H; NH_{Fca}), 8.29 (d, J = 7.1 Hz, 1H; NH_{Ala2}), 7.71 (d, J = 8.1 Hz, 1H; NH_{Ala1}), 4.76 (s, 1H; H-2, Fn), 4.68 (s, 1H; H-5, Fn), 4.45 (m, 1H; CH_{Ala1}), 4.39 (m, 2H; H-2′, H-5′, Fn), 4.31 (m, 1H; CH_{Ala2}), 4.24 (s, 2H; H-3, H-4, Fn), 3.93 (s, 2H; H-3′, H-4′, Fn), 3.61 (s, 3H; OCH_3), 1.33 (s, 9H; $C(CH_3)_3$), 1.24 ppm (m, 6H; 2CH_{3Ala}); ^{1}H NMR ($CDCl_3$): δ = 7.28 (s, 1H; NH_{Fca}), 7.01 (s, 1H; NH_{Ala1}), 6.90 (s, 1H; NH_{Ala2}), 4.70–4.00 (m, 10H; 2CH_{Ala}, Fn), 3.75 (s, 3H; OCH_3), 1.49 (s, 9H; $C(CH_3)_3$), 1.43 (s, 3H; CH_{3Ala}), 1.25 ppm (s, 3H; CH_{3Ala}); ^{13}C NMR ([D$_6$]DMSO): δ = 173.0 (COOCH$_3$), 172.8 (CO_{Ala1}), 168.7 (CO_{Fca}), 153.1 (COOtBu), 97.9 (C-1′, Fn), 78.6 ($C(CH_3)_3$), 76.4 (C-1, Fn), 71.2 (C-2 C-5, Fn), 68.9 (C-3′ C-4′, Fn), 65.4 (C-3 C-4, Fn), 61.3 (C-2′ C-5′, Fn), 51.8 (OCH_3), 47.9 (CH_{Ala2}), 47.5 (CH_{Ala1}), 28.1 ($C(CH_3)_3$), 17.9 (CH_{3Ala2}), 16.8 ppm (CH_{3Ala1}); IR (CH_2Cl_2): $\tilde{\nu}$ = 3428 (m, N-H free), 3309 (m, N-H assoc.), 1738 (s, C=O, $COOCH_3$), 1726 (s), 1711 (s), 1678 (s), 1658 (s), 1643 (s), 1632 cm^{-1} (s, C=O, COOtBu), (C=O, CONH); EIMS: m/z: 501 (27) $[M]^+$, 427 (34) $[M-t\text{BuOH}]^+$, 401 (61) $[H_2NFeCOAlaAlaOMe]^+$, 270 (36), 254 (43), 229 (100); ESI-MS (MeOH/CH_2Cl_2 10:1+0.1% trifluoroacetic acid (TFA)): m/z: 502.3 $[M+H]^+$; elemental analysis calcd (%) for $C_{23}H_{31}O_6N_3Fe$ (501.2): C 55.12, H 6.24, N 8.39; found: C 55.08, H 6.20, N 8.43.

Synthesis of Boc-Ala-Fca-Ala-OMe (20): This compound was prepared according to the procedure of the dipeptides **16–18**. Dipeptide **16** (437 mg, 1.02 mmol) was deprotected by gaseous HCl and evaporated in vacuo to dryness to leave yellow solid of H-Fca-Ala-OMe·HCl (350 mg, 94%), m.p. 80.2–83 °C. The resulting hydrochloride was treated with Et_3N in CH_2Cl_2 (pH ~ 8) and coupled with Boc-Ala-OH (361 mg, 1.91 mmol) by using the standard EDC/HOBt method. After stirring for 20 min and standard aqueous work-up, the crude material was purified by TLC (CH_2Cl_2/EtOAc, 10:1) to give yellow crystals (315 mg, 72%). M.p. 59–62 °C; ^{1}H NMR ([D$_6$]DMSO): δ = 9.24 (s, 1H; NH_{Fca}), 8.01 (d, J = 7.4 Hz, 1H; NH_{Ala1}), 7.04 (d, J = 10.5 Hz, 1H; $NH_{Ala1'}$), 4.77 (s, 1H; H-2, Fn), 4.70 (m, 1H; H-5, Fn), 4.62 (brs, 2H; H-2′, H-5′, Fn), 4.40 (t, J = 14.5 Hz, 1H; CH_{Ala}), 4.26 (m, 2H; H-3, H-4, Fn), 3.98 (m, 2H; H-3′, H-4′, Fn), 3.93 (t, J = 13.9 Hz, 1H; CH_{Ala}), 3.65 (s, 3H; OCH_3), 1.39 (s, 9H; $C(CH_3)_3$), 1.36 (brs, 3H; CH_{3Ala}), 1.20 ppm (d, J = 7.1 Hz, 3H; CH_{3Ala}); ^{1}H NMR ($CDCl_3$): δ = 9.12 (s, 1H; NH_{Fca}), 7.81 (d, 1H; NH_{Ala1}), 5.13 (d, 1H; $NH_{Ala1'}$), 5.36 (s, 1H; CH_{Ala}), 5.33 (s, 1H; CH_{Ala}), 4.91–4.02 (m, 8H; Fn), 3.85 (s, 3H; OCH_3), 1.30 (s, 3H; CH_{3Ala}), 1.40 ppm (brs, 12H; $C(CH_3)_3$, CH_{3Ala}); ^{13}C NMR ([D$_6$]DMSO): δ = 173.6 ($COOCH_3$), 171.6 ($CO_{Ala1'}$), 168.9 (CO_{Fca}), 155.2 (COOtBu), 96.2 (C-1′, Fn), 78.1 ($C(CH_3)_3$), 75.8 (C-1, Fn), 71.7 (C-2, Fn), 71.6 (C-5, Fn), 69.1 (C-3′, Fn), 68.8 (C-4′, Fn), 65.7 (C-3 C-4, Fn), 62.1 (C-2′, Fn), 61.5 (C-5′, Fn), 51.9 (OCH_3), 50.4 (CH_{Ala}), 47.6 (CH_{Ala}), 28.2 ($C(CH_3)_3$), 17.7 (CH_{3Ala}), 16.8 ppm (CH_{3Ala}); IR (CH_2Cl_2): $\tilde{\nu}$ = 3438 (w, N-H free), 3373 (m, N-H assoc.), 3322 (m, N-H assoc.), 1729 (s, C=O, $COOCH_3$), 1696 (s, C=O, COOtBu), 1648 cm^{-1} (s, C=O, CONH); EIMS: m/z: 501 (92) $[M]^+$, 445 (100) $[M-H_2CC(CH_3)_2]^+$, 401 (34) [AlaNHCpFeCpCOAlaOMe]$^+$, 330 (81) $[M-$AlaBoc+H$]^+$, 254 (44) [COCpFeCpNHCO]$^+$, 130 (28) [COAlaOMe]$^+$; ESI-MS (MeOH): m/z: 502.3 $[M+H]^+$; elemental analysis calcd (%) for $C_{23}H_{31}O_6N_3Fe$ (501.2): C 55.12, H 6.24, N 8.39; found: C 55.15, H 6.29, N 8.33.

Synthesis of Boc-Ala-Fca-Ala-Ala-OMe (21): After deprotection of the tripeptide **19** (420 mg, 0.8 mmol) by gaseous HCl in CH_2Cl_2, followed by evaporation, the resulting hydrochloride was treated with Et_3N in CH_2Cl_2 (pH ~ 8) and coupled with Boc-Ala-OH (139 mg, 0.74 mmol) by using the EDC/HOBt method followed by the standard aqueous work-up. TLC purification of the crude product (CH_2Cl_2/EtOAc, 10:1) results in a yellow crystalline material (130 mg, 65%). M.p. 94–97 °C;[15] ^{1}H NMR ([D$_6$]DMSO): δ = 10.02 (s, 1H; NH_{Fca}), 8.59 (d, 1H; NH_{Ala1}), 7.77 (d, 1H; NH_{Ala2}), 7.25 (d, 1H; $NH_{Ala1'}$), 4.85 (s, 1H; H-2, Fn), 4.74 (t, 1H; H-5, Fn), 4.67 (brs, 2H; H-2′, H-5′, Fn), 4.50 (m, 1H; CH_{Ala2}), 4.33 (s, 1H; CH_{Ala1}), 4.26 (s, 1H; H-4, Fn), 4.23 (s, 1H; H-3′, Fn), 4.02 (m, 1H; H-3, Fn), 3.93 (s, 1H; H-4′, Fn), 3.88 (m, 1H; $CH_{Ala1'}$), 3.61 (s, 3H; OCH_3), 1.40 (s, 9H; $C(CH_3)_3$), 1.33 (dd, 6H; 2CH_{3Ala}), 1.18 ppm (s, 3H; $CH_{3Ala1'}$); ^{1}H NMR ($CDCl_3$): δ = 9.86 (s, 1H; NH_{Fca}), 7.96 (d, 1H; NH_{Ala2}), 7.11 (d, 1H; NH_{Ala1}), 5.17 (d, 1H; $NH_{Ala1'}$), 5.20–4.00 (m, 11H; 3CH_{Ala}, Fc-CH), 3.77 (s, 3H; OCH_3), 1.55 (s, 3H; CH_{3Ala}), 1.47 (s, 12H; CH_{3Ala}, $C(CH_3)$), 1.37 ppm (s, 3H; CH_{3Ala}); ^{13}C NMR ([D$_6$]DMSO): δ = 174.0 ($COOCH_3$), 172.8 (CO_{Ala1}), 171.6 ($CO_{Ala1'}$, 168.7 (CO_{Fca}), 96.1 (C-1′, Fn), 78.4 ($C(CH_3)_3$), 75.9 (C-1, Fn), 71.7 (C-2, Fn), 70.8 (C-5, Fn), 69.4 (C-3′, Fn), 69.0 (C-4′, Fn), 65.2 (C-3 C-4, Fn), 62.5 (C-2′, Fn), 61.6 (C-5′, Fn), 54.8 (CH_{Ala}), 51.7 (OCH_3), 47.8 (2CH_{Ala}), 28.2 ($C(CH_3)_3$), 17.7 (CH_{3Ala}), 17.3 (CH_{3Ala}), 16.7 ppm (CH_{3Ala}); IR (CH_2Cl_2): $\tilde{\nu}$ = 3436 (m, N-H free), 3368, 3283, 3251 (m, N-H assoc.), 1742 (s, C=O, $COOCH_3$), 1695 (s), 1667 (s), 1642 (s), 1528 cm^{-1} (s, C=O, COOtBu), (C=O, CONH); EIMS: m/z: 572 (36) $[M]^+$, 516 (34) $[M-H_2CC(CH_3)_2]^+$, 501 (9), 498 (35) $[M-t\text{BuOH}]^+$, 401 (27) $[H_3NFeCOAlaAlaOMe]^+$, 325 (45), 270 (19), 254 (38), 229 (54), 130 (22), 57 (100); ESI-MS (MeOH/CH_2Cl_2 10:1+0.1% TFA): m/z: 573.3 $[M+H]^+$.

Synthesis of Boc-Ala-Ala-Fca-Ala-Ala-OMe (22): Pentapeptide **22** was prepared from H-Fca-Ala-Ala-OMe·HCl (180 mg, 0.51 mmol), which was treated with Et_3N and coupled with Boc-Ala-Ala-OH (264 mg, 1.01 mmol) as described above. TLC (CH_2Cl_2/EtOAc, 3:1) gave yellow crystals (120 mg, 39%). M.p. 99–102 °C; ^{1}H NMR ([D$_6$]DMSO): δ = 9.61 (s, 1H; NH_{Fca}), 8.53 (d, J = 6.9 Hz, 1H; NH_{Ala2}), 8.12 (d, J = 5.9 Hz, 1H; $NH_{Ala1'}$), 7.87 (d, J = 7.5 Hz, 1H; NH_{Ala1}), 7.00 (d, J = 6.9 Hz, 1H; $NH_{Ala2'}$), 4.79 (s, 1H; Fn), 4.74 (s, 1H; Fn), 4.67 (brs, 1H; Fn), 4.48 (m, 1H; CH_{Ala1}), 4.35 (m, 1H; CH_{Ala2}), 4.31 (m, 1H; Fn), 4.28 (s, 1H; Fn), 4.21 (s, 1H; Fn), 4.13 (s, 1H; $CH_{Ala1'}$), 4.01 (s, 1H; Fn), 3.98 (m, 1H; $CH_{Ala2'}$), 3.92 (s, 1H; Fn), 3.61 (s, 3H; OCH_3), 1.37 (s, 9H; $C(CH_3)_3$), 1.34 (d, J = 7.3 Hz, 3H; CH_{3Ala2}), 1.31 (d, J = 7.3 Hz, 3H; CH_{3Ala1}), 1.26 (d, J = 7.0 Hz, 3H; $CH_{3Ala1'}$), 1.21 ppm (d, J = 7.1 Hz, 3H; $CH_{3Ala2'}$); ^{1}H NMR ($CDCl_3$): δ = 9.78 (s, 1H; NH_{Fca}), 8.06 (d, 1H; NH_{Ala2}), 7.20 (brs, 1H; $NH_{Ala1'}$), 7.03 (brs, 1H; NH_{Ala1}), 5.28 (s, 1H; $NH_{Ala2'}$), 4.88–3.95 ((m, 12H; 4CH_{Ala}, Fc-H), 3.78 (s, 3H; OCH_3), 1.46 ppm (s, 21H; C-$(CH_3)_3$, 4CH_{3Ala}); ^{13}C NMR ([D$_6$]DMSO): δ = 174.0 (COOCH$_3$), 173.0 (CO_{Ala1}), 172.8 ($CO_{Ala2'}$), 170.8 ($CO_{Ala1'}$), 168.6 (CO_{Fca}), 155.0 (COOtBu), 95.9 (C-1′, Fn), 77.9 ($C(CH_3)_3$), 75.9 (C-1, Fn), 71.7 (C-2, Fn), 70.7 (C-5, Fn), 69.6 (C-3′, Fn), 68.9 (C-4′, Fn), 65.4 (C-3, Fn), 65.2 (C-4, Fn), 62.5 (C-2′, Fn), 61.6 (C-5′, Fn), 51.7 (OCH_3), 49.3 ($CH_{Ala2'}$), 49.1 ($CH_{Ala1'}$), 47.8 (CH_{Ala1}), 47.7 (CH_{Ala2}), 28.1 ($C(CH_3)_3$), 17.7 ($CH_{3Ala2'}$), 17.6 ($CH_{3Ala1'}$), 17.5 (CH_{3Ala1}), 16.7 ppm (CH_{3Ala2}); IR (CH_2Cl_2): $\tilde{\nu}$ = 3426 (m, N-H free), 3355, 3320 (w, N-H assoc.), 3296, 3251 (w, N-H assoc.), 1742 (s, C=O, $COOCH_3$), 1721 (s), 1710 (s), 1673 (s), 1692 (s), 1643 (s), 1632 (s), 1513 cm^{-1} (s, C=O, COOtBu), (C=O, CONH); EIMS: m/z: 643 (3) $[M]^+$, 569 (100) $[M-t\text{BuOH}]^+$, 543 (10) [AlaAlaFeCOAlaAlaOMe]$^+$, 396 (19), 270 (19), 304 (42), 229 (16) [Cp$_2$FeNHCO]$^+$; ESI-MS (MeOH/CH_2Cl_2 10:1+0.1% TFA): m/z: 644.5 $[M+H]^+$; elemental analysis calcd (%) for $C_{29}H_{41}O_8N_5Fe$ (643.2): C 54.15, H 6.43, N 10.89; found: C 54.13, H 6.47, N 10.93.

Synthesis of Boc-D-Ala-Fca-Ala-OMe (23): This compound was prepared as described above by using HBTU as a coupling reagent. Boc-Fca-Ala-OMe (430 mg, 1 mmol), Boc-Ala-OH (190 mg, 1 mmol), HBTU (418 mg, 1.1 mmol). Silica-gel column (hexane/EtOAc: 2:3, R_f = 0.33) to give yellow crystals (360 mg, 72%). ^{1}H NMR ($CDCl_3$): δ = 9.10 (s, 1H; CpNH), 7.35 (d, J = 7.8 Hz, 1H; NH_{DAla}), 5.40 (s, 1H; NH_{LAla}), 4.88 (m, 1H; NH_{LAla}), 4.63 (s, 1H; H-2, Cp), 4.57 (s, 1H; H-5, Cp), 4.52 (m, 1H; H^{α}_{DAla}), 4.47 (s, 1H; H-2′, Cp), 4.40 (s, 1H; H-5′, Cp), 4.34 (s, 1H; H-3, Cp), 4.29 (s, 1H; H-4, Cp), 4.02 (s, 1H; H-3′, Cp), 4.00 (s, 1H; H-4′, Cp), 3.78 (s, 3H; COOCH_3), 1.47 (s, 3H; CH_{3LAla}), 1.45 (s, 9H; C(CH_3)$_3$, Boc), 1.39 ppm (s, 3H; CH_{3DAla}); ^{1}H NMR ([D$_6$]DMSO, assignments based on COSY spectra): δ = 9.31 (s, 1H; FcNHCO), 8.06 (d, J = 6.5 Hz, 1H; NH_{DAla}), 7.04 (d, J = 5.6 Hz, 1H; NH_{LAla}), 4.77 (s, 1H; H_{Cp}), 4.74 (s, 1H; H_{Cp}), 4.69 (s, 1H; H_{Cp}), 4.53 (s, 1H; H_{Cp}), 4.40 (m, 1H; C$H_{\alpha LAla}$), 4.28 (s, 2H; H_{Cp}), 3.98 (s, 2H; H_{Cp}), 3.93 (m, 1H; C$H_{\alpha DAla2}$), 3.65 (s, 3H; COOCH_3), 1.40 (s, 9H; C(CH_3)$_3$), 1.38 (s, 3H; CH_{3LAla1}), 1.20 ppm (d, J = 7.7 Hz, 3H; CH_{3DAla2}); ^{13}C{^{1}H} NMR ($CDCl_3$): δ = 174.6 ($COOCH_3$), 171.4 ($CONH_{DAla}$), 170.1 (Cp$CONH_{LAla}$), 155.9 (CO, Boc), 95.0 (C-1′, Cp), 80.4 (C(CH_3)$_3$), 78.5 (C-1, Cp), 76.8 (C-2, Cp), 76.2 (C-5, Cp), 71.7 (C-2′, Cp), 71.2 (C-5′, Cp), 69.6 (C-3, Cp), 66.0 (C-4, Cp), 64.0 (C-3′, Cp), 63.5 (C-4′, Cp), 52.6 (COOCH_3), 51.2 (C^{α}_{DAla}), 50.9 (C^{α}_{LAla}), 28.3 (C-$(CH_3)_3$), 18.2 (CH_{3DAla}), 16.9 ppm (CH_{3LAla}); FTIR (KBr): $\tilde{\nu}$ = 3301 (m, N-H), 1745, 1683 (m, C=O), 1637 (s, amid I), 1531 cm^{-1} (s, amid II); IR (CH_2Cl_2): $\tilde{\nu}$ = 3429 (m, N-H free), 3307 (brm, N-H, H-bonded), 1734 (s,

C=O), 1697 (s), 1653 (s), 1540 (s), 1521, 1507 cm^{-1} (s); UV/Vis: λ_{max} (ε) = 440 nm (247 $M^{-1}cm^{-1}$); EIMS (+vs): *m/z* calcd for $C_{23}H_{31}N_3O_6Fe$ $[M]^+$: 501.1562; found: 501.1565.

Synthesis of Boc-Ala-Fca-D-Ala-OMe (24): The synthesis procedure is similar to that of compound **23**. Silica-gel column (hexane/ethyl acetate: 2:3, R_f = 0.32) to give yellow crystals (390 mg, 78%). ^{1}H NMR ($CDCl_3$): δ = 8.55 (s, 1H; CpN*H*), 7.18 (d, *J* = 7.6 Hz, 1H; NH_{DAla}), 5.29 (s, 1H; NH_{LAla}), 4.92 (m, 1H; NH_{DAla}), 4.63 (s, 1H; *H*-2, Cp), 4.59 (s, 1H; *H*-5′, Cp), 4.52 (overlapping, m, 2H; H^{α}_{DAla}, *H*-2′, Cp), 4.43 (s, 1H; *H*-5′, Cp), 4.39 (s, 1H; *H*-3, Cp), 4.34 (s, 1H; *H*-4, Cp), 4.07 (s, 1H; *H*-3′, Cp), 4.04 (s, 1H; *H*-4′, Cp), 3.82 (s, 3H; COOCH_3), 1.56 (s, 3H; CH_{3DAla}), 1.47 (s, 9H; C(CH_3)$_3$, Boc), 1.41 ppm (s, 3H; CH_{3LAla}); ^{1}H NMR ([D$_6$]DMSO, assignments based on COSY spectra): δ = 9.31 (s, 1H; FcNHCO), 8.05 (d, *J* = 6.5 Hz, 1H; NH_{LAla}), 7.04 (d, *J* = 5.6 Hz, 1H; NH_{DAla}), 4.77 (s, 1H; H_{Cp}), 4.73 (s, 1H; H_{Cp}), 4.69 (s, 1H; H_{Cp}), 4.53 (s, 1H; H_{Cp}), 4.40 (m, 1H; C$H_{\alpha DAla}$), 4.30 (s, 2H; H_{Cp}), 4.00 (s, 2H; H_{Cp}), 3.95 (m, 1H; C$H_{\alpha LAla}$), 3.56 (s, 3H; COOCH_3), 1.38 (s, 9H; C(CH_3)$_3$), 1.37 (s, 3H; CH_{3DAla}), 1.20 ppm (s, 3H; CH_{3Ala}); ^{13}C{^{1}H} NMR ($CDCl_3$): δ = 174.6 (*C*OOCH$_3$), 171.6 (*C*ONH$_{LAla}$), 170.4 (Cp*C*ONH$_{DAla}$), 160.1 (*C*O, Boc), 94.3 (*C*-1′, Cp), 79.6 (*C*(CH$_3$)$_3$), 78.5 (*C*-1, Cp), 76.8 (*C*-2, Cp), 75.4 (*C*-5, Cp), 72.0 (*C*-2′, Cp), 71.2 (*C*-5′, Cp), 70.5 (*C*-3, Cp), 65.4 (*C*-4, Cp), 64.0 (*C*-3′, Cp), 63.4 (*C*-4′, Cp), 52.6 (COO*C*H$_3$), 51.4 (C^{α}_{LAla}), 50.9 (C^{α}_{DAla}), 28.3 (C(*C*H$_3$)$_3$), 18.1 (*C*H$_{3LAla}$), 16.8 ppm (*C*H$_{3DAla}$); FTIR (KBr): $\tilde{\nu}$ = 3299 (m, N-H), 1741, 1684 (s, C=O), 1637 (s, amid I), 1532 cm^{-1} (s, amid II); IR (CH_2Cl_2): $\tilde{\nu}$ = 3430 (m, N-H free), 3359, 3317 (N-H, H-bonded), 1741 (s, C=O), 1696 (s), 1636 (s), 1650 (s), 1563, 1503 cm^{-1} (s); UV/Vis: λ_{max} (ε) = 438 nm (241 $M^{-1}cm^{-1}$); EIMS (+vs): *m/z* calcd for $C_{23}H_{31}N_3O_6Fe$ $[M]^+$: 501.1562; found: 501.1579.

Synthesis of Boc-Ala-Fca-Ala-D-Ala-OMe (25): Aqueous NaOH solution (0.1 M, 12 mL) was added dropwise at 0°C for 30 min to the solution of Boc-Ala-Fca-Ala-OMe (**23**) (500 mg, 1 mmol) in THF (12 mL), then reacted at RT overnight. THF was evaporated and 50 mL water was added to the aqueous solution. Then the solution was washed with EtOAc (3× 20 mL). The aqueous solution and 100 mL EtOAC were poured into a flask and cooled to 0°C, then 0.1 M HCl was added slowly to the solution to achieve pH 1–2. The aqueous phase was washed with EtOAc (3× 100 mL) and dried over $NaSO_4$, then filtered and evaporated under reduced pressure in a rotorvap to give the free acid as an orange solid (448 mg, 92%). Boc-Ala-Fca-Ala-OH (245 mg, 0.5 mmol) was dissolved in dry dichloromethane (100 mL), and reacted with H-D-Ala-OMe. The procedure is similar to that of compound **23**. Silica-gel column (hexane/EtOAc: 1:3, R_f = 0.21) giving yellow crystals of compound **25** (214 mg, 75%). ^{1}H NMR ($CDCl_3$): δ = 9.41 (s, 1H; CpN*H*), 7.84 (d, *J* = 7.0 Hz, 1H; NH_{DAla}), 7.29 (d, *J* = 7.2 Hz, 1H; NH_{LAla1}), 5.31 (s, 1H; *H*-2, Cp), 5.10 (d, *J* = 7.0 Hz, 1H; NH_{LAla}), 4.80 (s, 1H; *H*-5, Cp), 4.70 (m, 1H; H^{α}_{DAla}), 4.58 (s, 1H; *H*-2′, Cp), 4.56 (overlapping, m, 2H; H^{α}_{DAla}, *H*-5′, Cp), 4.27 (s, 1H; *H*-3, Cp), 4.11 (s, 1H; *H*-4, Cp), 4.06 (s, 1H; *H*-3′, Cp), 4.00 (s, 1H; *H*-4′, Cp), 3.75 (s, 3H; COOCH_{3LAla2}), 1.52 (s, 3H; CH_{3DAla}), 1.45 (s, 9H; C(CH_3)$_3$, Boc), 1.42 (s, 3H; CH_{3LAla1}), 1.36 ppm (s, 3H; CH_{3DAla}); ^{1}H NMR ([D$_6$]DMSO, assignments based on COSY spectra): δ = 9.32 (s, 1H; FcNHCO), 8.28 (d, *J* = 6.7 Hz, 1H; NH_{DAla2}), 7.77 (d, *J* = 7.1 Hz, 1H; NH_{LAla1}), 7.01 (d, *J* = 6.1 Hz, 1H; NH_{LAla3}), 4.77 (s, 1H; H_{Cp}), 4.68 (s, 1H; H_{Cp}), 4.67 (s, 1H; H_{Cp}), 4.56 (s, 1H; H_{Cp}), 4.45 (m, 1H; C$H_{\alpha LAla1}$), 4.31 (m, 1H; C$H_{\alpha DAla2}$), 4.28 (s, 2H; H_{Cp}), 3.98 (s, 2H; H_{Cp}), 3.91 (m, 1H; C$H_{\alpha LAla3}$), 3.65 (s, 3H; COOCH_3), 1.39 (s, 9H; C(CH_3)$_3$), 1.34 (m, 6H; CH_{3LAla1}, CH_{3DAla2}), 1.21 ppm (d, *J* = 6.6 Hz, 3H; CH_{3LAla3}); ^{13}C{^{1}H} NMR ($CDCl_3$): δ = 173.4 (*C*OOCH$_3$), 171.5 (*C*ONH$_{DAla}$), 170.5 (Cp*C*ONH$_{LAla1}$), 156.4 (*C*ONH$_{LAla2}$), 95.3 (*C*-1′, Cp), 78.0 (*C*(CH$_3$)$_3$, Boc), 77.4 (*C*-1, Cp), 71.7 (*C*-2, Cp), 70.2 (*C*-5, Cp), 69.3 (*C*-2′, Cp), 69.0 (*C*-5′, Cp), 66.3 (*C*-3, Cp), 66.1 (*C*-4, Cp), 64.0 (*C*-3′, Cp), 62.9 (*C*-4′, Cp), 52.8 (COO*C*H$_3$), 50.2 (C^{α}_{LAla1}), 48.8 (C^{α}_{LAla1}), 47.2 (C^{α}_{DAla1}), 28.2 (C(*C*H$_3$)$_3$), 17.8 (*C*H$_{3LAla1}$), 17.5 (*C*H$_{3LAla2}$), 16.5 ppm (*C*H$_{3DAla}$); FTIR (KBr): $\tilde{\nu}$ = 3277 (m, N-H), 1724, 1683 (m, C=O), 1637 (s, amid I), 1531 cm^{-1} (s, amid II); IR (CH_2Cl_2): $\tilde{\nu}$ = 3433 (m, N-H free), 3328 (br m, N-H, H-bonded), 1716 (s, C=O), 1654 (s), 1538 (s), 1509 cm^{-1} (s); UV/Vis: λ_{max} (ε) = 445 nm (384 $M^{-1}cm^{-1}$); EIMS (+vs): *m/z* calcd for $C_{26}H_{36}N_4O_7Fe$ $[M]^+$: 572.1933; found: 572.1938.

Synthesis of Boc-Ala-Fca-D-Ala-D-Ala-OMe (26): The synthetic procedure is identical to that described for **25**. Silica-gel column (hexane/EtOAc: 1:3, R_f = 0.20) to get yellow crystals (205 mg, 73%). ^{1}H NMR ($CDCl_3$): δ = 8.61 (s, 1H; CpN*H*), 7.41 (d, *J* = 7.0 Hz, 1H; NH_{DAla2}), 7.18 (d, *J* = 7.2 Hz, 1H; NH_{LAla}), 5.38 (s, 1H; *H*-2, Cp), 5.14 (d, *J* = 7.0 Hz, 1H; NH_{LAla}), 4.80 (s, 1H; *H*-5, Cp), 4.73 (m, 1H; H^{α}_{DAla}), 4.65 (s, 1H; *H*-2′, Cp), 4.60 (overlapping, m, 2H; $H^{\alpha}_{DAla1, LAla}$), 4.47 (s, 2H; H-2′, *H*-5′, Cp), 4.39 (s, 1H; *H*-3, Cp), 4.36 (s, 1H; *H*-4, Cp), 4.20 (m, 1H; C$^{\alpha}_{DAla2}$), 4.05 (s, 2H; *H*-3′, *H*-4′, Cp), 3.77 (s, 3H; COOCH_3), 1.54 (s, 3H; CH_{3LAla}), 1.50 (s, 3H; CH_{3DAla1}), 1.48 (s, 9H; C(CH_3)$_3$, Boc), 1.42 ppm (s, 3H; CH_{3DAla2}); ^{1}H NMR ([D$_6$]DMSO, assignments based on COSY spectra): δ = 9.30 (s, 1H; FcNHCO), 8.27 (d, *J* = 6.6 Hz, 1H; NH_{DAla2}), 7.74 (d, *J* = 7.6 Hz, 1H; NH_{DAla1}), 7.00 (d, *J* = 5.4 Hz, 1H; NH_{LAla3}), 4.77 (s, 1H; H_{Cp}), 4.69 (s, 1H; H_{Cp}), 4.66 (s, 1H; H_{Cp}), 4.56 (s, 1H; H_{Cp}), 4.43 (m, 1H; C$H_{\alpha DAla1}$), 4.30 (m, 1H; C$H_{\alpha DAla2}$), 4.26 (s, 2H; H_{Cp}), 3.97 (s, 2H; H_{Cp}), 3.94 (m, 1H; C$H_{\alpha LAla3}$), 3.62 (s, 3H; COOCH_3), 1.39 (s, 9H; C(CH_3)$_3$), 1.33 (m, 6H; CH_{3DAla1}, CH_{3DAla2}), 1.21 ppm (d, *J* = 6.6 Hz, 3H; CH_{3LAla3}); ^{13}C{^{1}H} NMR ($CDCl_3$): δ = 173.3 (*C*OOCH$_3$), 171.6 (*C*ONH$_{DAla1}$), 170.5 (Cp*C*ONH$_{LAla}$), 155.9 (*C*ONH$_{DAla2}$), 94.9 (*C*-1′, Cp), 80.4 (*C*(CH$_3$)$_3$, Boc), 77.0 (*C*-1, Cp), 76.8 (*C*-2, Cp), 76.4 (*C*-5, Cp), 71.6 (*C*-2′, Cp), 70.0 (*C*-5′, Cp), 66.9 (*C*-3, Cp), 65.4 (*C*-4, Cp), 64.0 (*C*-3′, Cp), 63.3 (*C*-4′, Cp), 52.3 (COO*C*H$_3$), 50.8 (C^{α}_{DAla2}), 50.0 (C^{α}_{LAla}), 48.0 (C^{α}_{DAla1}), 28.4 (C(*C*H$_3$)$_3$), 18.4 (*C*H$_{3LAla}$), 17.9 (*C*H$_{3DAla2}$), 17.7 ppm (*C*H$_{3DAla1}$); FTIR (KBr): $\tilde{\nu}$ = 3289 (m, N-H), 1745, 1666 (m, C=O), 1635 (s, amid I), 1531 cm^{-1} (s, amid II); IR (CH_2Cl_2): 3426 (m, N-H free), 3307 (br m, (N-H, H-bonded), 1741 (s, C=O), 1685 (s), 1654 (s), 1558 (s), 1507 cm^{-1} (s); UV/Vis (MeCN): λ_{max} (ε) = 445 nm (384 $M^{-1}cm^{-1}$); EIMS (+vs): *m/z* calcd for $C_{26}H_{36}N_4O_7Fe$ $[M]^+$: 572.1933; found: 501.1579.

Synthesis of Boc-D-Ala-Ala-Fca-Ala-D-Ala-OMe (27): Boc-Ala-Fca-Ala-D-Ala-OMe (285 mg, 0.5 mmol), Boc-D-Ala-OH (85 mg, 0.5 mmol), HBTU (210 mg, 0.55 mmol). Silica-gel column (hexane/EtOAc/MeOH: 10:85:5, R_f = 0.12) to give a yellow solid (103 mg, 31%). ^{1}H NMR ($CDCl_3$): δ = 9.08 (s, 1H; CpN*H*), 7.83 (s, 1H; N*H*,), 7.28 (s, 1H; N*H*), 7.20 (s, 1H; N*H*), 5.37 (s, 1H; *H*-2, Cp), 5.20 (d, *J* = 7.0 Hz, 1H; N*H*), 4.86 (overlapping, 2*H*), 4.46 (s, 1H; Cp), 4.47 (s, 1H; Cp), 4.26 (overlapping, 2H), 4.17 (m, 1H), 4.11 (s, 2H), 3.91 (s, 1H), 3.82 (s, 3H; COOCH_3), 1.46 (overlapping, 12H; CH_{3Ala}, C(CH_3)$_3$, Boc), 1.43–1.42 ppm (overlapping, 9H; CH_{3Ala}); ^{1}H NMR ([D$_6$]DMSO, assignments based on COSY spectra): δ = 9.19 (s, 1H; FcNHCO), 8.30 (d, *J* = 5.8 Hz, 1H; NH_{DAla2}), 8.02 (d, *J* = 6.2 Hz, 1H; NH_{LAla4}), 7.73 (d, *J* = 6.8 Hz, 1H; NH_{LAla1}), 7.01 (d, *J* = 5.5 Hz, 1H; NH_{LAla3}), 4.78 (s, 1H; H_{Cp}), 4.71 (s, 1H; H_{Cp}), 4.66 (s, 1H; H_{Cp}), 4.57 (s, 1H; H_{Cp}), 4.43 (m, 1H; C$H_{\alpha LAla1}$), 4.30 (m, 2H; C$H_{\alpha DAla2}$, C$H_{\alpha DAla3}$), 4.25 (s, 2H; H_{Cp}), 3.99 (s, 2H; H_{Cp}), 3.98 (m, 1H; C$H_{\alpha LAla4}$), 3.62 (s, 3H; COOCH_3), 1.37 (s, 9H; C(CH_3)$_3$), 1.32 (m, 6H; CH_{3LAla1}, CH_{3DAla2}), 1.27 (d, *J* = 7.0 Hz, 3H; CH_{3LAla4}), 1.18 ppm (d, *J* = 7.0 Hz, 3H; CH_{3LAla3}); ^{13}C{^{1}H} NMR ($CDCl_3$): δ = 176.8 (*C*OOCH$_3$), 173.4, 170.9, 165.7,155.6 (*C*ONH), 95.3 (Cp), 80.3 (*C*(CH$_3$)$_3$, Boc), 72.4, 71.5, 70.7, 70.5, 70.0, 66.0, 65.8, 65.3, 64.4, 62.8 (Cp), 52.7 (COO*C*H$_3$), 50.4, 50.0, 48.5, 48.0 (C^{α}_{Ala}), 28.3 (C(*C*H$_3$)$_3$), 19.6, 18.2, 17.5, 17.3 ppm (*C*H$_{3Ala}$); FTIR (KBr): $\tilde{\nu}$ = 3287 (m, N-H), 1740, 1659 (m, C=O), 1634 (s, amid I), 1530 cm^{-1} (s, amid II); IR (CH_2Cl_2): $\tilde{\nu}$ = 3424 (m, N-H free), 3325 (br m, (N-H, H-bonded), 1742 (s, C=O), 1684 (s), 1670 (s), 1517 cm^{-1} (br s); UV/Vis: λ_{max} (ε) = 439 nm (416 $M^{-1}cm^{-1}$); EIMS (+vs): *m/z* calcd for $C_{29}H_{41}N_5O_8Fe$ $[M+1]^+$: 643.2304; found: 644.2370.

Synthesis of Boc-Ala-Ala-Fca-D-Ala-D-Ala-OMe (28): Identical procedure to **25**. Silica-gel column (hexane/EtOAc/MeOH: 10:85:5, R_f = 0.12) to give a yellow solid (137 mg, 43%). ^{1}H NMR ($CDCl_3$): δ = 9.27 (s, 1H; CpN*H*), 7.88 (s, 1H; N*H*), 7.28 (s, 1H; N*H*), 6.68 (s, 1H; N*H*), 5.18 (s, 1H; *H*-2, Cp), 4.95 (d, *J* = 7.0 Hz, 1H; N*H*), 4.87 (s, 1H), 4.68 (s, 1H), 4.53–4.50 (overlapping, 3*H*), 4.27 (overlapping, 3H), 4.10 (s, 2H), 3.90 (s, 1H), 3.76 (s, 3H; COOCH_3), 1.47 (overlapping, 12H; CH_{3Ala}, C(CH_3)$_3$, Boc), 1.43–1.38 ppm (overlapping, 9H; CH_{3Ala}); ^{13}C{^{1}H} NMR ($CDCl_3$): δ = 174.6 (*C*OOCH$_3$), 173.5, 170.9, 166.1, 156.4 (*C*ONH), 95.3 (Cp), 80.3 (*C*(CH$_3$)$_3$, Boc), 72.0, 71.5, 71.6, 70.4, 70.1, 66.5, 66.4, 66.1, 64.4, 63.8 (Cp), 52.9 (COO*C*H$_3$), 51.3, 50.3, 48.9, 48.6 (C^{α}_{Ala}), 28.7 (C(*C*H$_3$)$_3$), 18.3, 18.2, 17.9, 17.8 ppm (*C*H$_{3Ala}$); FTIR (KBr): $\tilde{\nu}$ = 3293 (m, N-H), 1742, 1668 (s, C=O), 1629 (s, amid I), 1527 cm^{-1} (s, amid II); UV/Vis (MeCN): λ_{max} (ε) = 448 nm (323 $M^{-1}cm^{-1}$); EIMS (+vs): *m/z* calcd for $C_{29}H_{41}N_5O_8Fe$ $[M+1]^+$: 644.2304; found: 644.2379.

X-ray crystallographic data collection and refinement of the structures: X-ray data were collected by using a Bruker AXS CCD difractometer (graphite monochromated $Mo_{K\alpha}$ radiation, $\alpha = 0.71073$ Å) at 103 K and corrected for absorption (SADABS). The structures were solved by direct methods and refined on F^2 by using all reflections (SHELXTL).[21] Non-hydrogen atoms were refined anisotropically. Most of the hydrogen atoms (except some methyl hydrogen atoms in **21**) were located and refined isotropically. Tetrapeptide **21** crystallizes with a solvent molecule (probably pentane) that is severely disordered and could not be refined satisfactorily. Therefore, the data were corrected by using the SQUEEZE routine in PLATON.[22] The data are listed in Table 4. CCDC 297171–297173 (**16**–**18**) and 239828 (**21**) contain the supplementary crystallographic data for this paper. These data can be obtained free of charge from The Cambridge Crystallographic Data Centre via www.ccdc.cam.ac.uk/data_request/cif.

Acknowledgements

Experimental help by H. Rudy (MS and elemental analysis), U. Hertle, and W. Haseloff (NMR) is gratefully acknowledged. This work was supported in part by the Ministry of Science, Education, and Sport of Croatia (Zagreb group), the National Science and Engineering Research Council of Canada (Saskatoon group), the Canada Foundation for Innovation and the Saskatchewan Innovation Fund (Saskatoon group), the DFG (Heidelberg group), the Volkswagen Foundation (SIK), and a fellowship by the DAAD (L.B.). H.B.K. holds the Canada Research Chair in Biomaterials.

[1] a) S. G. Zhang, *Nat. Biotechnol.* **2003**, *21*, 1171–1178; b) V. Balzani, A. Credi, F. M. Raymo, J. F. Stoddart, *Angew. Chem.* **2000**, *112*, 3484–3530; *Angew. Chem. Int. Ed.* **2000**, *39*, 3348–3391.

[2] M. A. Shogren-Knaak, P. J. Alaimo, K. M. Shokat, *Annu. Rev. Cell Dev. Biol.* **2001**, *17*, 405–433.

[3] T. Moriuchi, T. Hirao, *Chem. Soc. Rev.* **2004**, *33*, 294–301.

[4] R. S. Herrick, R. M. Jarret, T. P. Curran, D. R. Dragoli, M. B. Flaherty, S. E. Lindyberg, R. A. Slate, L. C. Thornton, *Tetrahedron Lett.* **1996**, *37*, 5289–5292.

[5] For recent reviews, see: a) D. R. van Staveren, N. Metzler-Nolte, *Chem. Rev.* **2004**, *104*, 5931–5985; b) S. I. Kirin, H.-B. Kraatz, N. Metzler-Nolte, *Chem. Soc. Rev.* **2006**, *35*, 348–354.

[6] a) M. J. Sheehy, J. F. Gallagher, M. Yamashita, Y. Ida, J. White-Colangelo, J. Johnson, R. Orlando, P. T. M. Kenny, *J. Organomet. Chem.* **2004**, *689*, 1511–1520; b) D. Savage, G. Malone, J. F. Gallagher, Y. Ida, P. T. M. Kenny, *J. Organomet. Chem.* **2005**, *690*, 383–393.

[7] a) A. Nomoto, T. Moriuchi, S. Yamazaki, A. Ogawa, T. Hirao, *Chem. Commun.* **1998**, 1963–1964; b) T. Moriuchi, A. Nomoto, K. Yoshida, A. Ogawa, T. Hirao, *J. Am. Chem. Soc.* **2001**, *123*, 68–75; c) T. Moriuchi, A. Nomoto, K. Yoshida, T. Hirao, *Organometallics* **2001**, *20*, 1008–1013; d) T. Moriuchi, K. Yoshida, T. Hirao, *Org. Lett.* **2003**, *5*, 4285–4288; e) T. Moriuchi, K. Yoshida, T. Hirao, *J. Organomet. Chem.* **2003**, *668*, 31–34; f) T. Moriuchi, T. Nagai, T. Hirao, *Org. Lett.* **2005**, *7*, 5265–5268; g) T. Moriuchi, T. Nagai, T. Hirao, *Org. Lett.* **2006**, *8*, 31–34.

[8] a) Y. Xu, P. Saweczko, H.-B. Kraatz, *J. Organomet. Chem.* **2001**, *637–639*, 335–342; b) Y. Xu, H.-B. Kraatz, *Tetrahedron Lett.* **2001**, *42*, 2601–2603; c) F. E. Appoh, T. C. Sutherland, H.-B. Kraatz, *J. Organomet. Chem.* **2004**, *689*, 4669–4677; d) F. E. Appoh, T. C. Sutherland, H.-B. Kraatz, *J. Organomet. Chem.* **2005**, *690*, 1209–1217.

[9] a) D. R. van Staveren, T. Weyhermüller, N. Metzler-Nolte, *Dalton Trans.* **2003**, 210–220; b) X. de Hatten, T. Weyhermüller, N. Metzler-Nolte, *J. Organomet. Chem.* **2004**, *689*, 4856–4867; c) S. I. Kirin, D. Wissenbach, N. Metzler-Nolte, *New J. Chem.* **2005**, *29*, 1168–1173.

[10] a) K. Heinze, M. Schlenker, *Eur. J. Inorg. Chem.* **2004**, 2974–2988; b) K. Heinze, M. Schlenker, *Eur. J. Inorg. Chem.* **2005**, 66–71; c) K. Heinze, M. Beckmann, *Eur. J. Inorg. Chem.* **2005**, 3450–3457.

[11] a) S. Chowdhury, G. Schatte, H.-B. Kraatz, *Dalton Trans.* **2004**, 1726–1730; b) S. Chowdhury, K. A. Mahmoud, G. Schatte, H.-B. Kraatz, *Org. Biomol. Chem.* **2005**, *3*, 3018–3023; c) S. Chowdhury,

Table 4. Crystallographic data for **16**–**18**, and **21**.

Compound	**16**	**17**	**18**	**21**
empirical formula	$C_{20}H_{26}FeN_2O_5$	$C_{20}H_{26}FeN_2O_5$	$C_{20}H_{26}FeN_2O_5$	$C_{31}H_{48}FeN_4O_7$
formula weight	430.28	430.28	430.28	644.58
crystal size [mm]	0.46×0.15×0.06	0.33×0.20×0.07	0.30×0.07×0.03	0.27×0.20×0.11
crystal system	orthorhombic	orthorhombic	orthorhombic	orthorhombic
space group	$P2_12_12_1$	$P2_12_12_1$	$P2_12_12_1$	$P2_12_12_1$
a [Å]	7.4524(9)	7.4490(3)	7.7376(4)	11.2239(5)
b [Å]	16.196(2)	16.2143(7)	8.7815(4)	14.8020(7)
c [Å]	16.274(2)	16.2807(7)	30.0055(14)	18.6314(8)
α [°]	90	90	90	90
β [°]	90	90	90	90
γ [°]	90	90	90	90
V [Å^3]	1964.3(4)	1966.39(14)	2038.81(17)	3095.3(2)
Z	4	4	4	4
ρ_{calcd} [g cm^{-3}]	1.455	1.453	1.402	1.383
μ [mm^{-1}]	0.802	0.801	0.773	0.540
$F(000)$	904	904	904	1376
θ range for data collection [°]	1.77–32.03	1.77–32.05	2.42–32.03	1.76–30.51
index ranges	±10, 0–23, 0–24	±11, 0–23, 0–23	±11, 0–13, 0–44	±16, 0–21, 0–26
reflns collected	35357	18963	28165	27588
independent reflns	6752 [R(int) = 0.0424]	6692 [R(int) = 0.0369]	7056 [R(int) = 0.0505]	9445 [R(int) = 0.0484]
parameters	357	357	357	488
goodness-of-fit on F^2	1.049	1.046	1.056	1.059
final R indices [$I > 2\sigma(I)$]	$R1 = 0.0283$	$R1 = 0.0332$	$R1 = 0.0361$	$R1 = 0.0456$
	$wR2 = 0.0682$	$wR2 = 0.0734$	$wR2 = 0.0796$	$wR2 = 0.1043$
R indices (all data)	$R1 = 0.0335$	$R1 = 0.0426$	$R1 = 0.0483$	$R1 = 0.0657$
	$wR2 = 0.0712$	$wR2 = 0.0784$	$wR2 = 0.0861$	$wR2 = 0.1149$
absolute structure parameter	0.000(9)	−0.007(11)	−0.001(12)	−0.029(13)
largest diff. peak/hole [e Å^{-3}]	0.490/−0.254	0.602/−0.253	0.494/−0.318	0.661/−0.416

D. A. R. Sanders, G. Schatte, H.-B. Kraatz, *Angew. Chem.* **2006**, *118*, 765–768; *Angew. Chem. Int. Ed.* **2006**, *45*, 751–754; .

[12] a) J. T. Yli-Kauhaluoma, J. A. Ashley, C.-H. Lo, L. Tucker, M. M. Wolfe, K. D. Janda, *J. Am. Chem. Soc.* **1995**, *117*, 7041–7047; b) A. Heine, E. A. Stura, J. T. Yli-Kauhaluoma, C. Gao, Q. Deng, B. R. Beno, K. N. Houk, K. D. Janda, I. A. Wilson, *Science* **1998**, *279*, 1934–1940; c) C. E. Cannizzaro, J. A. Ashley, K. D. Janda, K. N. Houk, *J. Am. Chem. Soc.* **2003**, *125*, 2489–2506.

[13] Other synthetic pathways to Fca: a) I. R. Butler, S. C. Quayle, *J. Organomet. Chem.* **1998**, *552*, 63–68; b) T. Okamura, K. Sakauye, N. Ueyama, A. Nakamura, *Inorg. Chem.* **1998**, *37*, 6731–6736; and references [10a, 12a, 14a].

[14] a) L. Barišić, V. Rapić, V. Kovač, *Croat. Chem. Acta* **2002**, *75*, 199–210; b) G. Pavlović, L. Barišić, V. Rapić, I. Leban, *Acta Crystallogr. Sect. E* **2002**, *58*, m13–m15; c) G. Pavlović, L. Barišić, V. Rapić, V. Kovač, *Acta Cryst. Sect. C* **2003**, *59*, m55–m57; d) L. Barišić, V. Rapić, H. Pritzkow, G. Pavlović, I. Nemet, *J. Organomet. Chem.* **2003**, *682*, 131–142.

[15] L. Barišić, M. Dropučić, V. Rapić, H. Pritzkow, S. I. Kirin, N. Metzler-Nolte, *Chem. Commun.* **2004**, 2004–2005.

[16] D. W. Hall, J. H. Richards, *J. Org. Chem.* **1963**, *28*, 1549–1554.

[17] a) B. Ishimoto, K. Tonan, S. Ikawa, *Spectrochim. Acta Part A* **1999**, *56*, 201–209; b) Y. Jin, K. Tonan, S. Ikawa, *Spectrochim. Acta Part A* **2002**, *58*, 2795–2802; c) K. Tonan, S. Ikawa, *Spectrochim. Acta Part A* **2003**, *59*, 111–120.

[18] N. Metzler-Nolte in *Bioorganometallics* (Ed.: G. Jaouen), Wiley-VCH, Weinheim, **2005**, pp. 125–179.

[19] a) A. Rodger, B. Norden, *Circular Dichroism and Linear Dichroism*, Oxford University Press, Oxford, UK, **1997**; b) S. M. Kelly, T. J. Jess, N. C. Price, *Biochim. Biophys. Acta* **2005**, *1751*, 119–139.

[20] W. Bauer, K. Polborn, W. Beck, *J. Organomet. Chem.* **1999**, *579*, 269–279.

[21] G. M. Sheldrick, SHELXTL V5.1, Bruker AXS, Madison, Wisconsin, **1998**.

[22] A. L. Spek, PLATON, Utrecht University, **1980–2005**.

Received: February 3, 2006
Published online: May 24, 2006

